TI Designs
Magnetic Tamper Detection Using Low-Power Hall Effect Sensors

TI Designs

This design implements a Class 0.2 three-phase energy measurement system that detects magnetic tampering using Hall sensors. The TIDA-00839 detects magnetic tampering when running from both main and backup power sources. This design reduces the current consumption of the Hall sensors to increase battery life when running from the backup power source.

Design Resources

TIDA-00839	Design Folder
DRV5033	Product Folder
UCC28910	Product Folder
TPS54060	Product Folder
ISO7320	Product Folder
TRS3232	Product Folder
TPS70933	Product Folder
ISO7321	Product Folder
MSP430F67791A	Product Folder

TI E2E™ Community — ASK Our E2E Experts

Design Features

- Multiple Omnipolar Hall Sensors Monitor Energy Measurement CTs and SMPS Transformers to Detect Magnetic Attacks
- Sensor B_{OP} = ±6.9 mT, Sensor B_{RP} = ±3.5 mT
- SMPS or Cap-Drop Power Supply Options
- Support for Backup Power Sources
- Software Power Duty-Cycling Reduces Current Consumption per Sensor to < 2 µA
- Case Tamper Detection Capability
- Three-Phase Energy Measurement Exceeds Class 0.2 Accuracy Requirements From ANSI and IEC
- Option for Programmable Penalty for Detected Magnetic Fields
- TI Energy Library Firmware Calculates All Energy Measurement Parameters Including Active and Reactive Power; Active and Reactive Energy; Root Mean Square (RMS) Current and Voltage; Power Factor; and Line Frequency

Featured Applications

- Metering

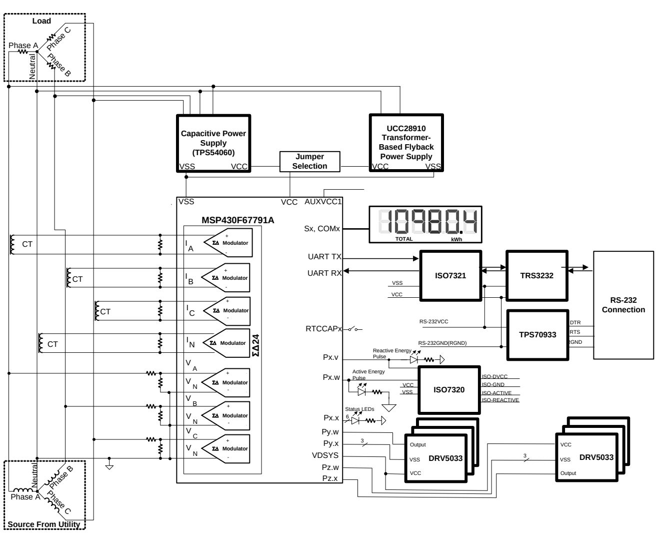

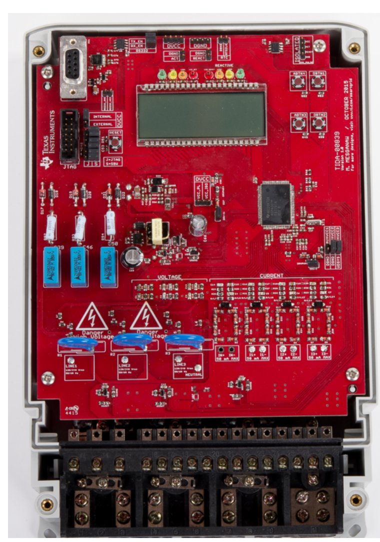

An IMPORTANT NOTICE at the end of this TI reference design addresses authorized use, intellectual property matters and other important disclaimers and information.

1 System Description

In an energy measurement system, transformers may be used in the system's power supply or as the system's current sensors. A disadvantage of using transformers is that magnetic fields could cause transformer cores to saturate, thereby rendering them useless. For a transformer used in a power supply, this may lead to the system being unable to be powered normally. For current transformer current sensors specifically, this may prevent properly registering the current drawn by a customer's load, thereby leading to undercharging a customer for energy consumption. Due to this magnetic susceptibility of transformers, tamperers may purposely subject a system to a magnet in an attempt to paralyze the system. One way of addressing magnetic tampering is to measure the magnetic field and take the necessary actions when a high magnetic field is detected.

This design implements an ANSI/IEC Class 0.2 accuracy three-phase energy measurement system that uses the DRV5033 Hall effect sensors for detecting magnetic tampering. This design is for a three-phase energy measurement system, but it can also be scaled down for a single-phase system.

This system uses an energy measurement system on chip (SoC) to sense current and voltage, calculate metrology parameters, drive a 160-segment LCD, and communicate to a PC GUI through the board's isolated RS-232 circuitry. As an additional tamper detection feature, this SoC can detect attempts to open the system's case to physically tamper with the system.

In this application, whenever there is a detected magnetic field there is an option that would allow penalizing a customer for this high magnetic field. This penalty is accomplished by calculating metrology parameters with a large, user-defined current instead of calculating metrology parameters using the current actually sensed.

To deal with the magnetic susceptibility of transformer-based supplies, it is common for energy measurement systems to use cap-drop supplies that do not use transformers. However, for systems that draw a large current from the power supply, using a transformer in the power supply may be unavoidable. This design supports using both a cap-drop or transformer power supply through its TPS54060 capacitive-based power supply and its UCC28910 transformer-based power supply. For the transformer-based power supply, there are Hall effect sensors near the transformer to detect magnetic tamper attempts near the power supply transformer. If the transformer is paralyzed by a magnetic tamper event and the main power is lost, the system can switch to a backup power source to allow the system to still be functional. Since the backup power source may be a battery, it is important to reduce the current consumption of the Hall sensors to maximize battery life cycle. This current consumption reduction is accomplished by duty cycling the power to each Hall sensor as in the white paper *Sub-Microamp, Intelligent Hall-Effect Sensing Delivers 20-Year Battery Life* [1].

In regards to metrology, the software energy library supports calculating various parameters for up to three-phase energy measurement. The key parameters calculated during energy measurements are: RMS current and voltage, active and reactive power and energies, power factor, and frequency. These parameters can be viewed either from the calibration GUI or LCD. This design guide has a complete metrology source code provided as a downloadable zip file.

1.1 DRV5033

The DRV5033 is a Hall effect sensor that detects magnetic tampering. These sensors are omnipolar, so they could respond to either the south pole or north pole of a magnet. A strong magnetic field of either polarity causes the output to pull low (operate point, B_{OP}), and a weaker magnetic field causes the output to release (release point, B_{RP}) , as shown in Figure 1.

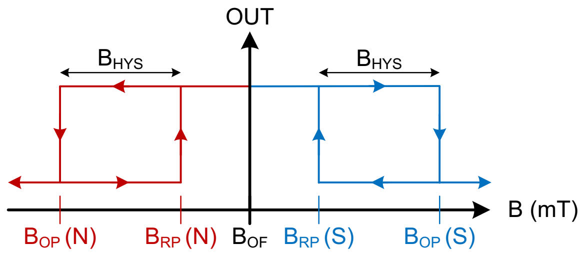

Figure 1. DRV5033 Output State

This design uses two sets of three sensors. Because these sensors have an open drain output, the outputs of the multiple sensors can simply be directly connected to each other. The shared output would indicate whether or not a magnetic field is detected on any of the multiple Hall sensors. The first set of sensors is oriented so that there is one sensor near each current transformer. The second set of three sensors is placed near the power supply transformer (near the center of the board). For this particular set of sensors, each sensor is oriented so that it could sense magnetic tampering in all three dimensions. For sensing in three dimensions, two SIP package DRV sensors are used with one SOT23 package DRV sensor.

1.2 UCC28910

The UCC28910 is used in the transformer-based power supply to help provide a 3.3-V output from an input mains voltage of 100- to 240-V AC_{RMS} at 50 or 60 Hz. Figure 8 shows how the UCC28910 is used to create the 3.3-V output from the 100- to 240-V AC_{RMS} input. To detect a magnetic tamper event near the transformer in this power supply, a set of three Hall sensors are used (one for each direction).

1.3 TPS54060

The TPS54060 is used in the capacitive-based power supply to provide a 3.3-V output from an input mains voltage of 100- to 240-V AC_{RMS} at 50 or 60 Hz. Figure 7 shows the TPS54060-based power supply, which outputs 3.3-V using a 100- to 240-V AC_{RMS} input.

1.4 ISO7321

To add isolation to the RS-232 connection to a PC, the isolated RS-232 portion of this design uses capacitive galvanic isolation, which has an inherent lifespan advantage over an opto-isolator. In particular, industrial devices are usually pressed into service for much longer periods of time than consumer electronics; therefore, maintenance of effective isolation over a period of 15 years or longer is important.

The TI ISO7321 is a simple dual-channel isolator that is capable of operating at 3.3 V or 5 V, enabling a wide range of devices that can connect to the data circuit-terminating equipment (DCE) side of the interface. The ISO7321 can simply be inserted into a universal asynchronous receiver/transmitter (UART) signal path, with the appropriate power supplies on each side to enable operation. The ISO7321 also maintains 3 kV of isolation to meet the Underwriters Laboratories (UL) certification levels.

The ISO7321 is available as ISO7321C and ISO7321FC variants, and the difference of these variants is in whether the default output is high or low, respectively. Although both variants can be used in the design, this design specifically uses the ISO7321C.

1.5 TRS3232

To properly interface with the RS-232 standard, a voltage translation system is required to convert between the 3.3-V domain on the board and from the 12 V on the port itself. To facilitate the translation, the design uses the TRS3232. The TRS3232 is capable of driving the higher voltage signals on the RS-232 port from only the 3.3-V DVCC through a charge pump system.

1.6 TPS70933

To power the data terminal equipment (DTE) side of the isolation boundary and the RS-232 charge pump, there are two choices: The interface can either implement an isolated power supply or harvest power from the RS-232 line. Integrating a power supply adds cost and complexity to the system, which is difficult to justify in low-cost sensing applications.

To implement the second option of harvesting power from the RS-232 port itself, this design uses the flow control lines that are ignored in most embedded applications. The RS-232 specification (when properly implemented on a host computer or adapter cable), keeps the request to send (RTS) and data terminal ready (DTR) lines high when the port is active. As long as the host has the COM port open, these two lines retain voltage on them. This voltage can vary from 5 to 12 V, depending on the driver implementation. The 5 to 12 V is sufficient for the use requirements in this design.

The voltage is put through a diode arrangement to block signals from entering back into the pins. The voltage charges a capacitor to store energy. The capacitor releases this energy when the barrier and charge pump pull more current than what is instantaneously allowed. The TPS70933 brings the line voltage down to a working voltage for the charge pump and isolation device.

1.7 ISO7320

To test the active energy and reactive energy accuracy of a system, pulses are output at a rate proportional to the amount of energy consumed. A reference meter can then determine the accuracy of an energy measurement system by calculating the error based on these pulses and how much energy is provided to the system. In this design, pulses are output through headers for the cumulative active and reactive energy consumption. Using the ISO7320 provides an isolated version of these headers for connection to non-isolated equipment. These isolated active and reactive signals can be set to have either a 3.3- or 5-V maximum voltage output by applying the selected maximum voltage output between the isolated sides VCC (ISO_VCC) and the isolated sides GND (ISO_GND).

The ISO7320 is available as ISO7320C and ISO7320FC variants, where the difference of these variants is in whether the default output is high or low. Although both variants can be used in the design, this design specifically uses the ISO7320C.

1.8 MSP430F67791A

To sense and calculate the metrology parameters, this design uses the MSP430F67791A energy measurement SoC. This device is the latest metering SoC that belongs to the MSP430F67xxA family of devices.

The MSP430F67791A drives a 160-segment LCD and communicates to a PC GUI through the board's isolated RS-232 circuitry. In addition, the chip has a real-time clock (RTC) module that keeps track of date and time and automatically logs case tamper events.

Also, by using the AUX module on the F67791A, this device and the DRV sensors can operate when the transformer-based power supply is paralyzed from a high magnetic field. Figure 2 shows the block diagram of this AUX module.

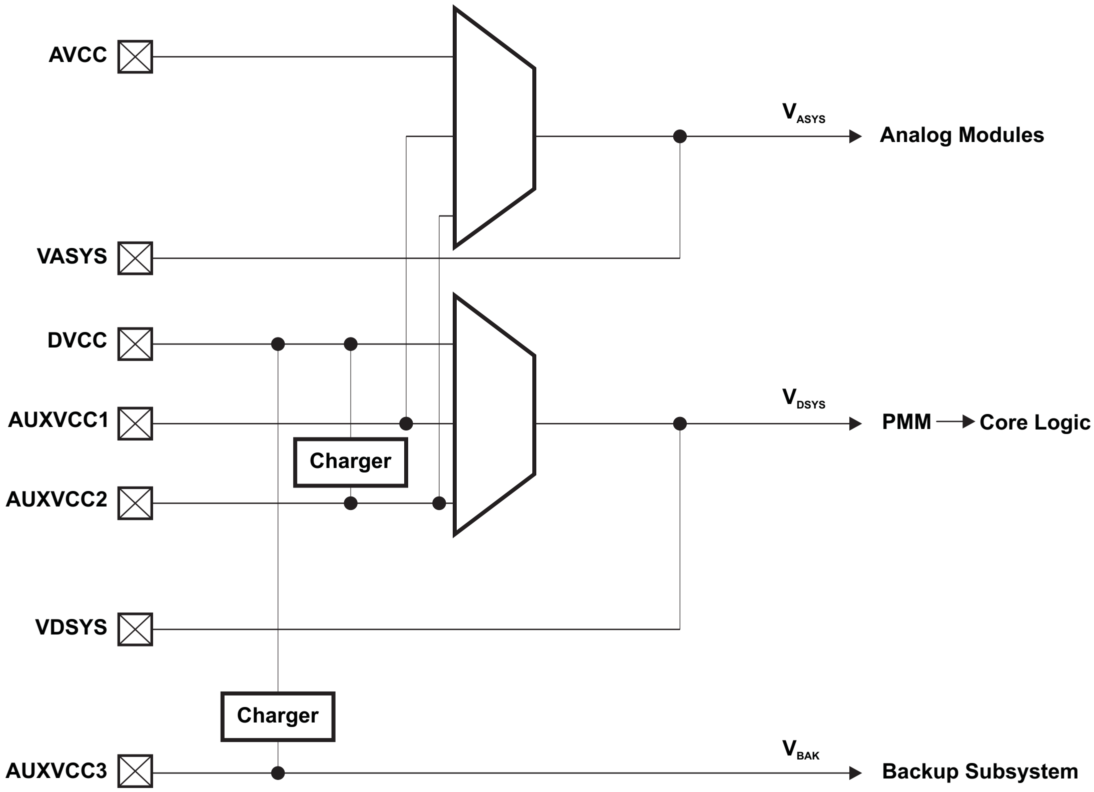

Figure 2. MSP430F67791A AUX Module Block Diagram

In this module, VDSYS and VASYS power the chip. In this application, VDSYS and VASYS are either connected to DVCC/AVCC or AUXVCC1. Specifically, this module is configured so that whenever the main power at DVCC or AVCC falls below a certain threshold, the entire chip switches to being powered by the power source at AUXVCC1 (assuming AUXVCC1 is available). Because the VDSYS pin is connected to the DRV5033 sensors and the current draw from the DRV5033 chips is low, whichever supply powers the chip also powers the DRV sensors so that magnetic tampering can still be detected even when the transformer in the power supply is paralyzed. For more information on this AUX module, please see the TIDM-AUX-MODULE design guide (TIDU452).

In addition to detecting magnetic tamper (with the DRV5033) and case tamper events, the MSP430F67791A also has an extra ADC channel in addition to the ones used for sensing phase voltages and phase currents. This extra ADC channel can be used to sense the neutral current to detect tampering by attempting to bypass current.

2 Block Diagram

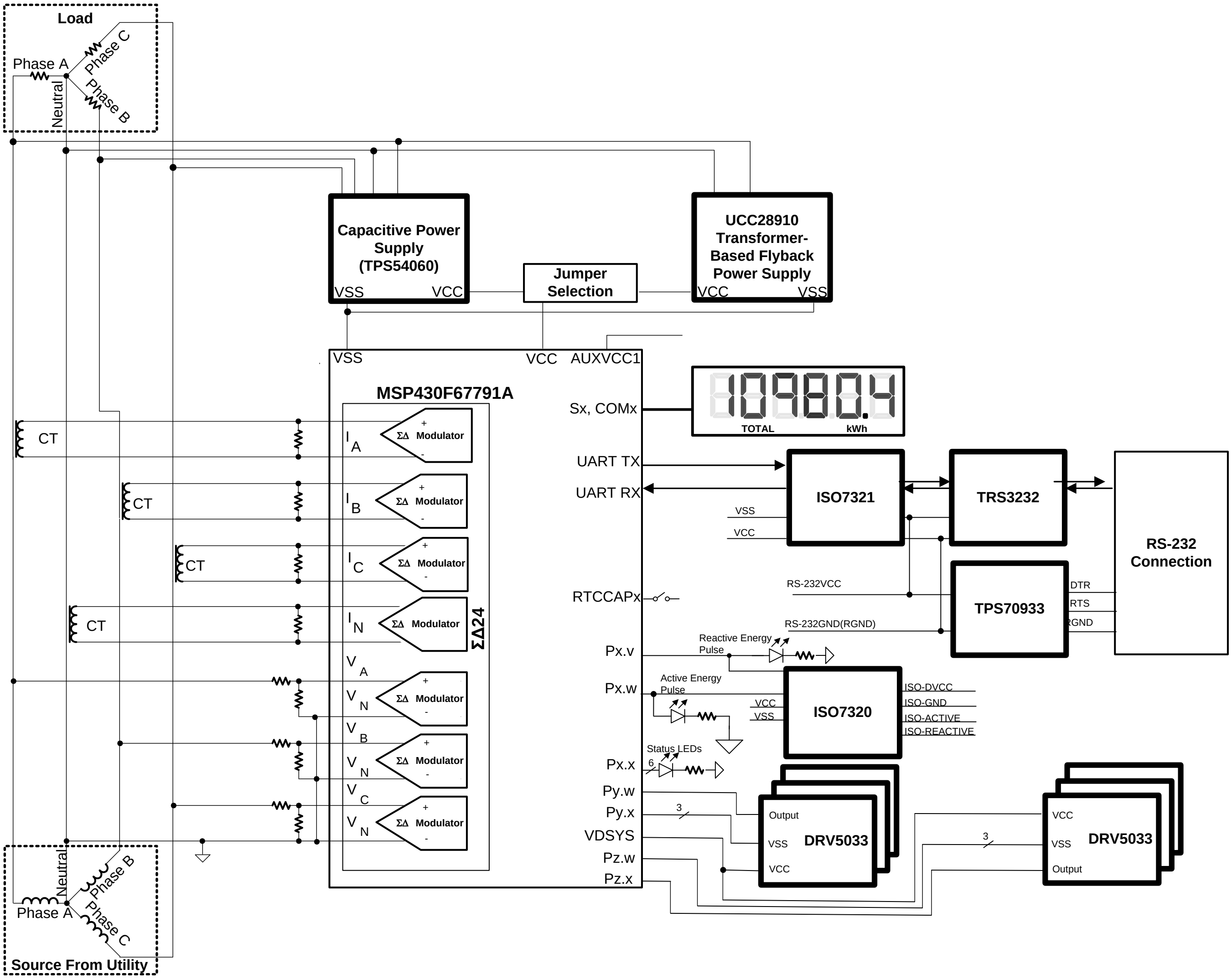

Figure 3. System Block Diagram

Figure 3 displays the high-level interface used for a three-phase energy measurement application that uses the MSP430F67791A. In this case, this figure shows a three-phase, four-wire star connection to the AC mains. In the diagram, current sensors are connected to each of the current channels, and a simple voltage divider is used for corresponding voltages. The CT has an associated burden resistor that has to be connected at all times to protect the measuring device. The choice of the CT and the burden resistor is done based on the manufacturer and current range required for energy measurements. The choice of voltage divider resistors for the voltage channel is selected to ensure the mains voltage is divided down to adhere to the normal input ranges that are valid for the MSP430ΣΔ24. Refer to the MSP4305xx/6xx user's guide (SLAU208) and device specific datasheet (SLAS983) for these numbers.

For tamper detection, case tampering and magnetic tampering are supported. For case tamper detection, a switch that is triggered whenever the case is opened is connected to one of the RTCCAP pins. Whenever the switch is triggered, the time and date of the tamper event is automatically logged. For this system, this switch is simulated using one of the push buttons on the board.

In magnetic tamper detection, two sets of three DRV5033 sensors are used. One set of sensors detects magnetic tamper events near the current transformers, and the other sensor set senses tamper events near the power supply transformer. All of the sensors have the MSP430F67791A's VDSYS signal (the supply used to power the chip) connected to VCC of the sensors. Also, within each set of DRV5033 sensors, the outputs of the three sensors are connected to each other (assuming the correct jumper settings are used). In contrast, the GND pin of each sensor is connected by default jumper settings to a different pin on the MSP430F67791A so that each DRV sensor can be enabled or disabled individually.

Figure 3 shows two options for the main power source—a cap-drop supply based on the TPS54060 and a transformer based supply using the UCC28910. When the transformer based supply is used and the transformer in the supply is paralyzed, the application automatically switches to powering the device and Hall sensors from the supply connected between AUXVCC1(+) and VSS(–).

Other signals of interest in Figure 3 are the status LEDs and the active/reactive energy pulses used to measure accuracy and calibrate the system. The ISO7320 provides an isolated connection for these pulses for connecting to non-isolated equipment. In addition to isolated pulses, the design supports isolated RS-232 communication through the use of the TPS70933, ISO7321, and TRS3232. Find more information on the isolated RS-232 portion of the design at http://www.ti.com/tool/TIDA-00163.

2.1 Highlighted Products

2.1.1 DRV5033

The DRV5033 is a chopper-stabilized Hall effect sensor that offers a magnetic sensing solution with superior sensitivity stability over temperature and integrated protection features.

The DRV5033 responds the same to both polarities of magnetic field direction. When the applied magnetic flux density exceeds the B_{OP} threshold, the DRV5033 open drain output goes low. The output stays low until the field decreases to less than B_{RP}, and then the output goes to high impedance. The output current sink capability is 30 mA. A wide operating voltage range from 2.5 to 38 V with reverse polarity protection up to –22 V makes the device suitable for a wide range of industrial applications.

Internal protection functions are provided for reverse supply conditions, load dump, and output short circuit or overcurrent. A summary of features of this device is as follows:

- Digital omnipolar-switch Hall sensor
- Superior temperature stability
  - B_{OP} ±10% over temperature
- High sensitivity (B_{OP} and B_{RP})
  - ±6.9 / ±3.5 mT (AJ)
- Detects north and south magnetic field
- Supports a wide voltage range
  - 2.5 to 38 V
  - No external regulator required
- Wide operating temperature range
  - T_A = –40 to 125°C (Q)
- Open drain output (30-mA sink)
- Fast 35-µs typical (50-µs maximum) power-on time
- Small package and footprint
  - Surface mount 3-pin SOT-23 (DBZ)
    - 2.92 × 2.37 mm
  - Through-hole 3-pin SIP (LPG)
    - 4.00 × 3.15 mm

2.1.2 UCC28910

The UCC28910 is a high-voltage flyback switcher that provides output voltage and current regulation without the use of an optical coupler. This device incorporate a 700-V power FET and a controller that process operating information from the flyback auxiliary winding and power FET to provide a precise output voltage and current control. The integrated high-voltage current source for startup, which is switched off during device operation, and the controller current consumption is dynamically adjusted with the load. Both enable the very low standby power consumption.

Combining switching frequency and peak primary current modulation, the control algorithms in the UCC28910 allow operating efficiencies to meet or exceed applicable standards. Discontinuous conduction mode (DCM) with valley switching reduces switching losses. Built-in protection features help to keep secondary and primary component stress levels in check across the operating range. The frequency jitter helps to reduce EMI filter cost. A summary of this device's feature is as follows:

- Constant-voltage (CV) and constant-current (CC) output regulation without optical-coupler
- ±5% output voltage regulation accuracy
- ±5% output current regulation with AC line and primary inductance tolerance compensation
- 700-V start-up and smart power management enables <30-mW standby power
- 115-kHz maximum switching frequency design for high-power density
- Valley switching and frequency dithering to ease EMI compliance
- Thermal shutdown
- Low line and output overvoltage protection

2.1.3 TPS54060

The TPS54060A is a 60-V, 0.5-A, step-down regulator with an integrated high-side MOSFET. Current mode control provides simple external compensation and flexible component selection. A low-ripple pulse skip mode reduces the no load, regulated output supply current to 116 µA. Using the enable pin, shutdown supply current is reduced to 1.3 µA when the enable pin is low.

Undervoltage lockout is internally set at 2.5 V, but can be increased using the enable pin. The output voltage startup ramp is controlled by the slow start pin that can also be configured for sequencing or tracking. An open-drain power good signal indicates the output is within 94% to 107% of its nominal voltage.

2.1.4 ISO7321

The ISO7321 provides galvanic isolation up to 3 kV_{RMS} for one minute per UL. This digital isolator has two isolated channels where one is a forward channel and the other is a reverse channel. Each isolation channel has a logic input and output buffer separated by a silicon dioxide (SiO2) insulation barrier. This chip supports a signaling rate of 25 Mbps. The chips can operate from 3.3- and 5-V supply and logic levels. At the rated voltage, the ISO7321 has over a 25-year isolation integrity.

2.1.5 TRS3232

The TRS3232 consists of two line drivers, two line receivers, and a dual charge-pump circuit with ±15-kV ESD protection pin to pin (serial-port connection pins, including GND). The device meets the requirements of TIA/EIA-232-F and provides the electrical interface between an asynchronous communication controller and the serial-port connector. The charge pump and four small external capacitors allow operation from a single 3- to 5.5-V supply. The devices operate at data signaling rates up to 250 kbps and a maximum of 30-V/µs driver output slew rate.

2.1.6 TPS70933

The TPS70933 linear regulator is a ultralow, quiescent current device designed for power-sensitive applications. A precision band-gap and error amplifier provides 2% accuracy over temperature. Quiescent current of only 1 µA makes these devices ideal solutions for battery-powered, always-on systems that require very little idle-state power dissipation. This device features thermal-shutdown, current-limit, and reverse-current protections for added safety.

2.1.7 ISO7320

The ISO7320 provides galvanic isolation up to 3 kV_{RMS} for 1 minute per UL. This digital isolator has two isolated forward channels. Each isolation channel has a logic input and output buffer separated by a silicon dioxide (SiO2) insulation barrier. This chip supports a signaling rate of 25 Mbps. The chips can operate from a 3.3- and 5-V supply and logic levels. At the rated voltage, the ISO7320 has over a 25-year isolation integrity.

2.1.8 MSP430F67791A

Figure 4 shows the features of the MSP430F67791A.

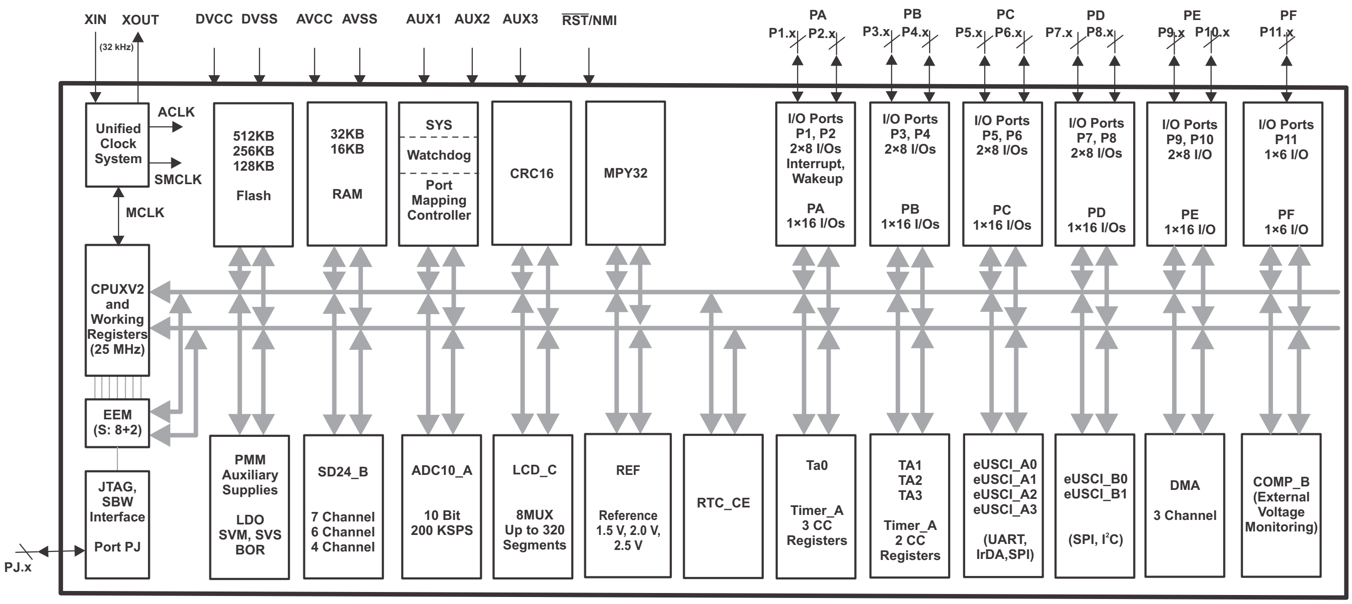

Figure 4. MSP430F67791A Block Diagram

Similar to the MSP430F67791, the MSP430F67791A belongs to the powerful 16-bit MSP430F6xx platform. This device finds its application in energy measurement and has the necessary architecture to support it. The MSP430F67791A has a powerful 25-MHz CPU with MSP430CPUx architecture. The analog front-end (AFE) consists of seven independent 24-bit ΣΔ analog-to-digital converters (ADCs) based on a second-order sigma-delta architecture that supports differential inputs. The sigma-delta ADCs (SD24_B) operate independently and are capable of 24-bit results. They can be grouped together for simultaneous sampling of voltages and currents on the same trigger. In addition, it also has an integrated gain stage to support gains up to 128 for amplification of low-output current sensors. A 32×32-bit hardware multiplier on this chip can further accelerate math intensive operations during energy computation.

The RTC module on this device supports both offset and temperature compensation to ensure accurate time keeping. Additionally, the RTC module supports automatic logging of an external event or tamper detection attempt. Other features of this chip include a module for switching between main and backup power sources.

3 System Design Theory

3.1 Design Hardware Implementation

3.1.1 Analog Inputs

The MSP430 AFE, which consists of the ΣΔ ADC, is differential and requires that the input voltages at the pins do not exceed ±930 mV (gain = 1). To meet this specification, the current and voltage inputs need to be divided down. In addition, the ΣΔ24 allows a maximum negative voltage of –1 V. Therefore, AC signals from mains can be directly interfaced without the need for level shifters.

3.1.1.1 Voltage Inputs

The voltage from the mains is usually 230 V or 120 V and for optimal accuracy is usually scaled down within 930 mV. In the AFE for voltage, there consists a spike protection varistor, EMI filter beads (which should help for ESD testing), a voltage divider network, and a RC low-pass filter that acts like an anti-alias filter.

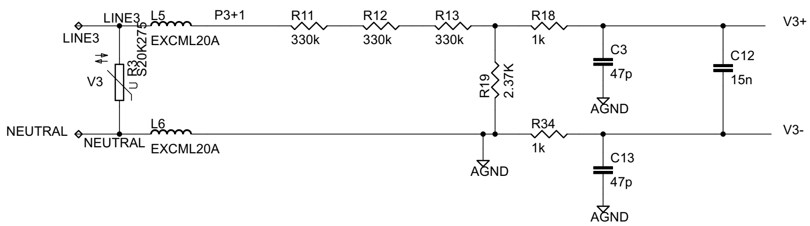

Figure 5. AFE for Voltage Inputs

Figure 5 shows the AFE for voltage inputs for a mains voltage of 230 V. The voltage is brought down to approximately 549 mV_{RMS}, which is 779 mV at its peak, and fed to the positive input. This voltage is within the MSP430ΣΔ analog limits by a safety margin greater than 15%. This margin allows accurate measurements even during voltage spike conditions. Additionally, note that the anti-alias resistors on the positive and negative sides are different because the input impedance to the positive terminal is much higher; therefore, a lower value resistor is used for the anti-alias filter. If this is not maintained, a relatively large phase shift would result.

3.1.1.2 Current Inputs

The AFE for current inputs is slightly different from the AFE for the voltage inputs. Figure 6 shows the AFE used for a current channel. The AFE for current consists of diodes and transorbs for transient voltage suppression (TVS). In addition, the front-end consists of EMI filter beads (which help for ESD testing), burden resistors for current transformers, and also an RC low-pass filter that acts like an anti-alias filter.

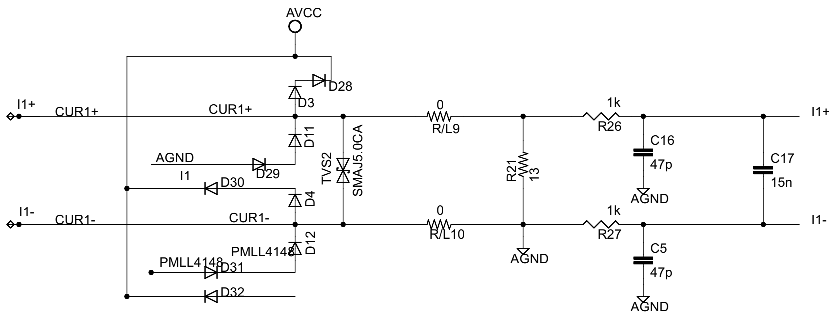

Figure 6. AFE for Current Inputs

In Figure 6, Resistor R104 is the burden resistor that would be selected based on the current range used and the turns ratio specification of the CT (CTs with a turns ratio of 2000:1 are used for this design). The value of the burden resistor for this design is around 13 Ω. The antialiasing circuitry, consisting of resistors and capacitors, follow the burden resistor. Based on this EVM's maximum current of 100 A, CT turns ratio of 2000:1, and burden resistor of 13 Ω, the input signal to the converter is a fully differential input with a voltage swing of ±919 mV maximum when the maximum current rating of the system (100 A) is applied. In addition, footprints for suppressant inductors are also available. These inductor footprints are shown below as R/L1 and R/L2 and by default are populated with 0-ohm resistors.

3.1.2 Power Supply

The MSP430 family of microcontrollers support a number of low-power modes in addition to low-power consumption during active (measurement) mode when the CPU and other peripherals are active. Because an energy meter is always interfaced to the AC mains, deriving the DC supply required for the measuring element (MSP430F67791A) is easy using an AC-to-DC conversion mechanism. The reduced power requirements of this device family allow design of power supplies to be small, extremely simple, and cost-effective. The power supply allows the operation of the energy meter by powering it directly from the mains.

3.1.2.1 Cap Drop Power Supply

Figure 7 shows a capacitor power supply that provides a single output voltage of 3.3 V directly from the mains of 100- to 240-V AC_{RMS} at 50 or 60 Hz.

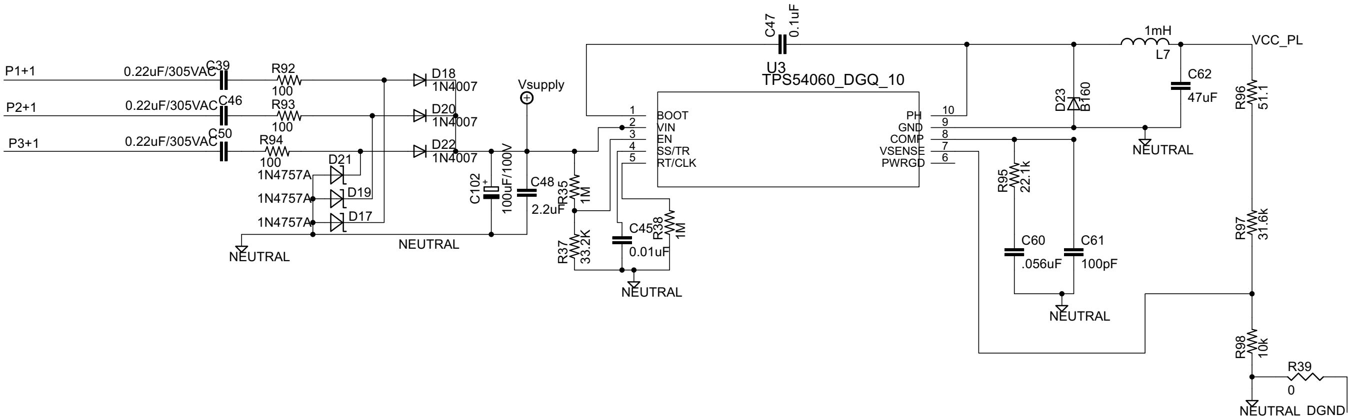

Figure 7. Simple Capacitive Power Supply for MSP430 Energy Meter

Appropriate values of resistors (R92, R93, and R94) and capacitors (C39, C46, and C50) are chosen based on the required output current drive of the power supply. Voltage from mains is directly fed to a RC-based circuit followed by a rectification circuitry to provide a DC voltage for the operation of the MSP430. This DC voltage is regulated to 3.3 V for full speed operation of the MSP430. The design equations for the power supply are given in the application report *Improved Load Current Capability for Cap-Drop Off-Line Power Supply for E-Meter* (SLVA491) .This configuration allows all three phases to contribute to the current drive, which is approximately three times the drive available from only one phase. If an even higher output drive is required, use the same circuitry followed by an NPN output buffer. Another option would be to replace the above circuitry with a transformer- or witching-based power supply.

3.1.2.2 Flyback Power Supply

Figure 8 shows a switching-based power supply that provides a single output voltage of 3.3 V directly from the AC mains 100- to 240-V_{RMS}. In Figure 8, the energy measurement system is powered as long as there is AC voltage on Phase C, corresponding to pad "LINE 3" on the HW and P3+1 on the schematic. A three-phase version of this supply can also be derived as shown in PMP9053.

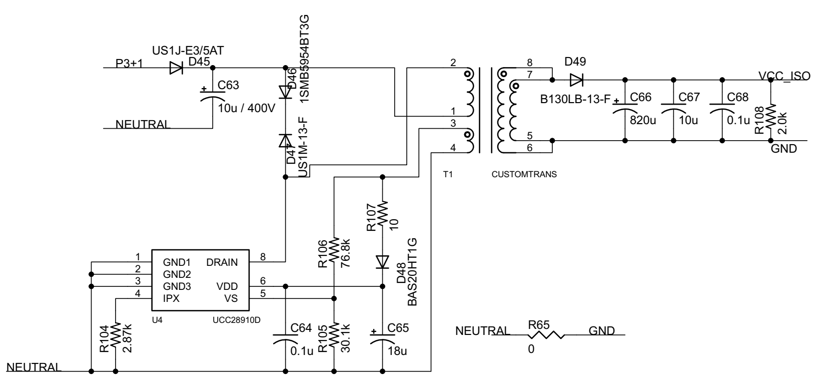

Figure 8. Flyback Power Supply for MSP430 Energy Meter

3.1.3 Magnetic Tamper Detection

The DRV5033 has a B_{OP} of ±6.9 mT and a B_{RP} of ±3.5 mT. For applications where these B_{OP} and B_{RP} settings are too sensitive for the magnetic flux density that the Hall sensor is actually exposed to, the sensitivity of these devices could be reduced by shielding the sensors.

Figure 9 shows the schematic for one of the two sets of Hall sensors. In the schematic, each DRV5033 is powered from VDSYS of the MSP430F67791A (assuming the correct jumper settings are used), thereby allowing the DRV5033 sensors to be powered from whichever supply (main or backup) is powering the MSP430F67791A. To measure the current consumption of the set of three Hall sensors, use the DRV-I1 jumper.

To reduce the average current consumption of each DRV sensor, the power to the DRV5033 sensor is duty cycled by connecting or disconnecting each sensor's GND pin. To allow each sensor to be enabled or disabled individually, each sensor's GND is connected to a different GPIO pin (assuming the correct jumper settings are used) on the MSP430F67791A.

Each Hall effect sensor shown in Figure 9 has an open-drain output that requires a pullup resistor (R45, R47, and R64) . Since all the outputs are open drain, the logical OR of magnetic status can be obtained by simply connecting the outputs together. In Figure 9, there is an option to connect the outputs of all the sensors in a set to one GPIO pin or connect each DRV sensor to a different GPIO pin by adjusting the position of the jumper resistors connected to the output. When the outputs of the DRV5033 in a set are connected, the pullup resistors are effectively in parallel leading to a pullup resistance of 10k. When they are not connected, the pullup resistances are not in parallel. As a result, the pullup resistors should be changed from 30k to 10k when the outputs of the DRV sensors are not connected to each other.

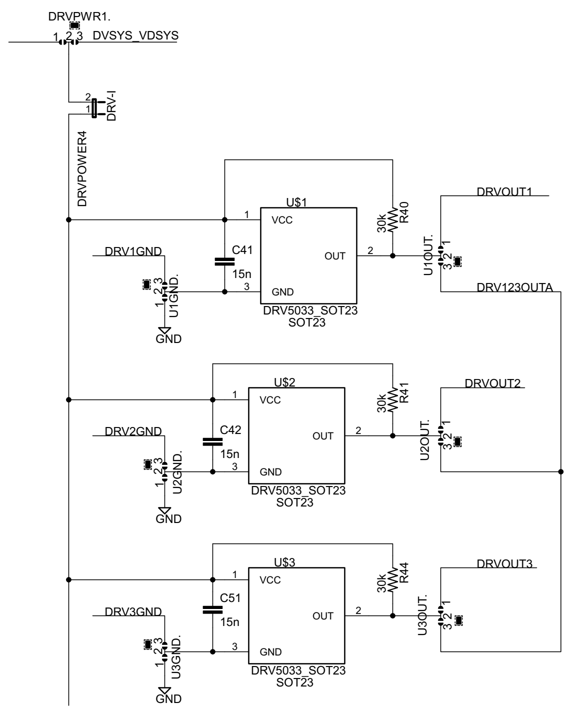

Figure 9. Set of Hall Sensors

3.2 Software Implementation

This section discusses the software for the implementation of three-phase metrology. The first subsection discusses the setup of various peripherals of the MSP430 device. Subsequently, this section describes the entire metrology software as two major processes: the foreground process and background process.

3.2.1 Peripherals Setup

The major peripherals of the MSP430F67791A are the 24-bit sigma delta (SD24_B) ADC, the auxiliary power supply module (AUX), clock system, RTC, LCD, and watchdog timer (WDT).

3.2.1.1 SD24_B Setup

For a three-phase system, at least six ΣΔs are necessary to independently measure three voltages and currents. The code accompanying this design guide addresses the metrology for a three-phase system with limited discussion to anti-tampering; however, the code supports the measurement of the neutral current.

The clock to the SD24_B (f_M) ADCs derives from the digitally controlled oscillator (DCO) running at 25 MHz. The sampling frequency is defined as $f_S = f_M$ / OSR, the oversampling ratio (OSR) is chosen to be 256, and the modulation frequency, f_M, is chosen as 1.048576 MHz, resulting in a sampling frequency of 4.096 samples per second. The SD24s are configured to generate regular interrupts every sampling instant.

The following are the ΣΔ channel associations:

- A0.0+ and A0.0– → Voltage V1
- A1.0+ and A1.0– → Voltage V2
- A2.0+ and A2.0– → Voltage V3
- A4.0+ and A4.0– → Current I1
- A5.0+ and A5.0– → Current I2
- A6.0+ and A6.0– → Current I3

Optional neutral channel can be processed through channel A3.0+ and A3.0–.

3.2.1.2 AUX Module

The AUX module is set so that hardware switching is enabled for DVCC and AUXVCC1. AUXVCC2 is disabled. In the software, the SVSMH voltage is set to level 5 because this level is above the 2.5 V necessary for the DRV5033 to function properly (see the MSP430F67791A datasheet (SLAS983) for the range of exact voltages that correspond to this particular level) . When VDSYS, the supply selected to power the chip, falls below this SVSMH level, the AUX module triggers for VDSYS to switch to another supply (as long as the supply to switch to is above a user-defined threshold). The OK-voltage threshold for AUXVCC1 (AUX1LVL) is level 5. The OK-voltage level for DVCC (AUX0LVL) is level 6. Note that if DVCC was previously not declared OK, but is later on, the AUX module switches to DVCC even if VDSYS is not below the SVSMH level. This auto-switch behavior is only true for DVCC and is not applicable for AUXVCC1 or AUXVCC2.

Whenever the supply powering the chip is switched from DVCC to AUXVCC1 or vice versa, the AUX module is configured to generate an interrupt to log this change so that it could later be decided to enter a low-power state with decreased functionality (if switched to AUXVCC1) or exit the low-power state and resume normal functionality (if switched to DVCC).

For more information about the AUX module, see the user's guide or the following TI design: http://www.ti.com/tool/TIDM-AUX-MODULE.

3.2.1.3 Real Time Clock (RTC_C)

The RTC_C is a RTC module that is configured to give precise one-second interrupts as well as keep track of the time and date. In addition, the RTC_C logs the time of the first tamper event detected on RTCCAP1. This tamper event is simulated by pressing the ABTN3 button on the board. To clear the current tamper event to detect the next tamper event, DBTN2 can be pressed whenever DVCC is available.

3.2.1.4 LCD Controller (LCD_C)

The LCD controller on the MSP430F67791A can support up to eight-mux displays and 320 segments. The LCD controller is also equipped with an internal charge pump that can be used for good contrast. In the current design, the LCD controller is configured to work in four-mux mode using 160 segments with a refresh rate set to ACLK/64, which is 512 Hz.

3.2.2 Foreground Process

The foreground process includes the initial setup of the MSP430 hardware and software immediately after a device RESET. Figure 10 shows the flowchart for this process. The initialization routines involve the setup of the ADC, clock system, auxiliary supply system, general purpose input and output (GPIO) port pins, RTC module for clock functionality, LCD, and the USCI_A0 for universal asynchronous receiver and transmitter (UART) functionality.

After the hardware is setup, any received frames from the GUI are processed. Once they are processed, the application checks whether the device’s power has just recently been switched to AUXVCC1 due to insufficient voltage at DVCC. Because AUXVCC1 may be connected to a battery, the current consumption of the system is reduced by the aux1_Mode_Prepare() function. This aux1_Mode_Prepare() function disables the RS-232 circuitry, disables all LEDs, disables the RTC 1-second interrupt (the RTC time-keeping functionality is still enabled though), reduces the active mode clock to approximately 4 MHz, disables the metrology so that there are no sigma-delta interrupts, selects the lowest internal core voltage setting, and enters LPM3 low-power mode.

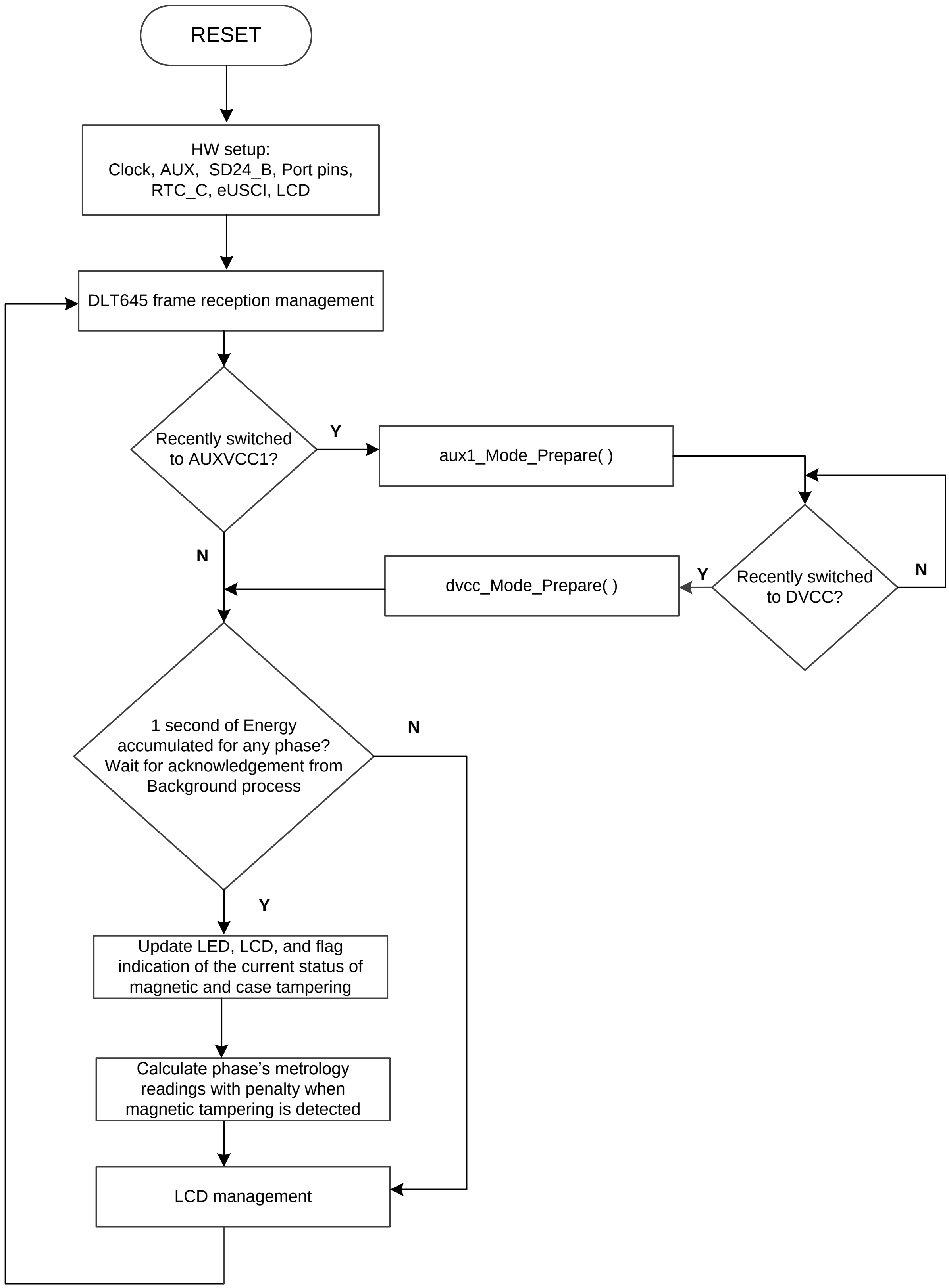

Figure 10. Foreground Process

When in the mode where AUXVCC1 is powering the chip, because the sigma-delta module is disabled and the CPU is only ON in an interrupt service routine, a timer interrupt updates the LCD with new parameters, turning ON the Hall sensors for magnetic tamper detection, and sensing the current state of the case tampering input pin. Figure 11 shows the flowchart for the timer interrupt.

As shown in Figure 11, the timer for sensing magnetic and case tampering is set to generate an interrupt at a rate of four times per second. For this particular case, only the set of DRV sensors near the transformer (DRV4, DRV5, and DRV6) are enabled because there is no need to sense near the current transformers, which is because metrology calculations would not be calculated while the system is powered from AUXVCC1. In addition, all sensors are turned ON at the same time to reduce the interrupt rate of the timer so that the MSP430F67791A could spend a longer time in LPM3. All of the sensors are turned ON for approximately 50 to 60 µs. With the ON time of 60 µs and a typical 2.7-mA current draw of the DRV5033, the current draw from one DRV5033 (with magnetic field not present) can be estimated as:

$$\mathrm{I\_measurement\_DRV5033} \times \text{Active duty cycle} = 2700\ \mu\text{A} \times \frac{\left(60 \times 10^{-6}\,\text{s}\right)}{0.25\ \text{s}} = 0.648\ \mu\text{A} \tag{1}$$

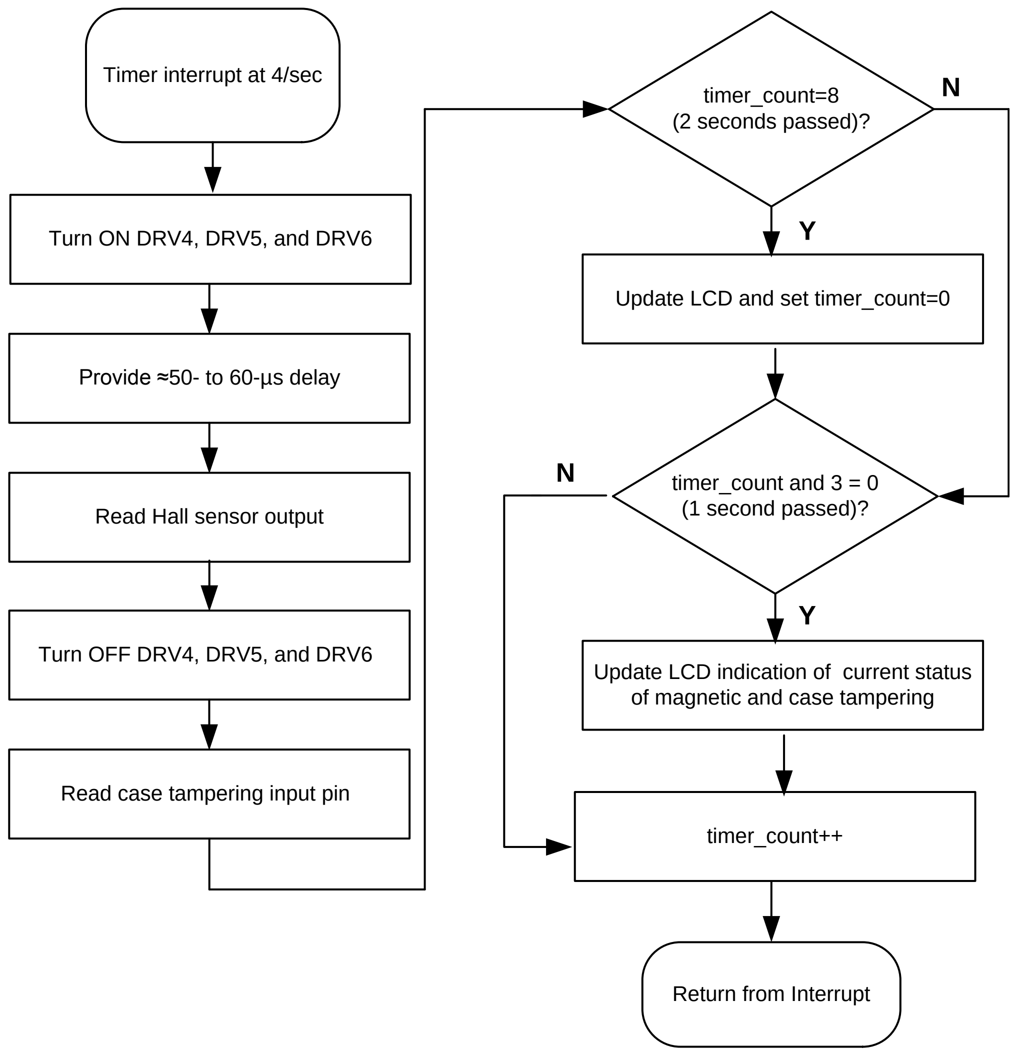

Figure 11. Timer Interrupt Flowchart

When the chip switches to being powered to DVCC, the MSP430F67791A exits from the LPM3 low-power mode and enters active mode. After entering active mode, the dvcc_Mode_Prepare() function is called to reverse the changes done by the aux1_Mode_Prepare function. These changes include re-enabling all LEDs, re-enabling the RS-232 circuitry, disabling the timer used for sampling the Hall sensors, increasing the CPU clock back to 25 MHz, and re-enabling the sigma-delta module to generate interrupts and calculate metrology parameters.

If the chip is being powered from DVCC, the foreground process checks whether the background process has notified the foreground process to calculate new metering parameters. This notification is accomplished through the assertion of the "PHASE_STATUS_NEW_LOG" status flag whenever a frame of data is available for processing. The data frame consists of the processed current, voltage, and active and reactive quantities that have been accumulated for one second. This accumulation is equivalent to an accumulation of 50 or 60 cycles of data synchronized to the incoming voltage signal. In addition, a sample counter keeps tracks of how many samples accumulate over this frame period. This count can vary as the software synchronizes with the incoming mains frequency.

The processed dot products include the V_{RMS}, I_{RMS}, active power, and reactive power. The foreground process uses these dot products to calculate the corresponding metrology readings in real-world units. Processed voltages accumulate in a 48-bit register. In contrast, processed currents, active energies, and reactive energies accumulate in separate 64-bit registers to further process and obtain the RMS and mean values. Using the calculated values of active and reactive power from the foreground, the apparent power is calculated. The frequency (in Hz) and power factor are also calculated using parameters calculated by the background process using the formulas in Section 3.2.2.1.

Whenever PHASE_STATUS_NEW_LOG is specifically asserted for Phase C, the LEDs LED1 to LED6 and LCD are updated to reflect the most recent status of the case and magnetic tamper detection. For the LED and LCD display of tamper detection state, a tamper detection event is declared for a frame of data when at least three out of the four previous results within the frame of data indicate a tamper event has occurred. After a user-defined consecutive number of frames that have magnetic tampering detected, a metrology penalty can be applied by assuming that the actual current drawn from a consumer’s load is equal to a large, user-defined penalty current instead of the actual measured current. For example, in this particular application, the penalty current is set to 100 A, so the RMS current would be set to 100 A and the active power set equal to (V_{RMS} × 100) W whenever there are a certain number of consecutive frames of magnetic tampering detected.

3.2.2.1 Formulae

This section briefly describes the formulas used for the voltage, current, energy, and temperature calculations.

As previous sections describe, voltage and current samples are obtained at a sampling rate of 4096 Hz. All of the samples that are taken in one second are kept and used to obtain the RMS values for voltage and current for each phase. The RMS values are obtained by the following formulas:

$$V_{RMS,ph} = K_{v,ph} \times \sqrt{\frac{\sum_{n=1}^{\text{Sample count}} v_{ph}(n) \times v_{ph}(n)}{\text{Sample count}} - v_{offset,ph}} \quad (2)$$

$$I_{RMS,ph} = K_{i,ph} \times \sqrt{\frac{\sum_{n=1}^{\text{Sample count}} i_{ph}(n) \times i_{ph}(n)}{\text{Sample count}} - i_{offset,ph}} \quad (3)$$

where

- ph = Phase parameters that are being calculated [that is, Phase A(= 1), B(= 2), or C(= 3)]
- $v_{ph}(n)$ = Voltage sample at a sample instant n
- $v_{offset,ph}$ = Offset used to subtract effects of the additive white Gaussian noise from the voltage converter
- $i_{ph}(n)$ = Each current sample at a sample instant n
- $i_{offset,ph}$ = Offset used to subtract effects of the additive white Gaussian noise from the current converter
- Sample count = Number of samples in one second
- $K_{v,ph}$ = Scaling factor for voltage
- $K_{i,ph}$ = Scaling factor for each current

Power and energy are calculated for a frame's worth of active and reactive energy samples. These samples are phase corrected and passed on to the foreground process, which uses the number of samples (sample count) to calculate phase active and reactive powers through the following formulas:

$$P_{ACT,ph} = K_{ACT,ph} \frac{\sum_{n=1}^{\text{Sample count}} v(n) \times i_{ph}(n)}{\text{Sample count}} \quad (4)$$

$$P_{REACT,ph} = K_{REACT,ph} \frac{\sum_{n=1}^{\text{Sample count}} v_{90}(n) \times i_{ph}(n)}{\text{Sample count}} \quad (5)$$

$$P_{APP,ph} = \sqrt{P_{ACT,ph}^{2} + P_{REACT,ph}^{2}} \quad (6)$$

where

- v_{90} (n) = Voltage sample at a sample instant ‘n’ shifted by 90°
- $K_{ACT,ph}$ = Scaling factor for active power
- $K_{REACT,ph}$ = Scaling factor for reactive power

Note that for reactive energy, the 90° phase shift approach is used for two reasons:

1. This approach accurately measures the reactive power for very small currents.
2. This approach conforms to the measurement method specified by IEC and ANSI standards.

The calculated mains frequency calculates the 90°-shifted voltage sample. Because the frequency of the mains varies, it is important to first measure the mains frequency accurately to phase shift the voltage samples accordingly (see Section 3.2.3.1.2 for details).

To get an exact 90° phase shift, interpolation is used between two samples. For these two samples, a voltage sample slightly more than 90° before the current sample is used, and a voltage sample slightly less than 90° before the current sample is used. The application's phase shift implementation consists of an integer part and a fractional part. The integer part is realized by providing an N samples delay. The fractional part is realized by a one-tap FIR filter. In the software, a lookup table provides the filter coefficients that are used to create the fractional delays.

In addition to calculating the per-phase active and reactive powers, the cumulative sum of these parameters are also calculated by Equation 7, Equation 8, and Equation 9:

$$P_{ACT,\,Cumulative} = \sum_{ph=1}^{3} P_{ACT,ph} \tag{7}$$

$$P_{REACT,\,Cumulative} = \sum_{ph=1}^{3} P_{REACT,ph} \tag{8}$$

$$P_{APP,\,Cumulative} = \sum_{ph=1}^{3} P_{APP,ph} \tag{9}$$

Using the calculated powers, energies are calculated by the following formulas:

$$E_{ACT,\,ph} = P_{ACT,\,ph} \times \text{Sample count} \tag{10}$$

$$E_{REACT,\,ph} = P_{REACT,\,ph} \times \text{Sample count} \tag{11}$$

$$E_{APP\ ph} = P_{APP\ ph} \times \text{Sample count} \tag{12}$$

From these equations, the energies are also accumulated to calculate the cumulative energies by Equation 13, Equation 14, and Equation 15:

$$E_{ACT,\,Cumulative} = \sum_{ph=1}^{3} E_{ACT,ph} \tag{13}$$

$$E_{REACT,\,Cumulative} = \sum_{ph=1}^{3} E_{REACT,ph} \tag{14}$$

$$E_{APP,\,Cumulative} = \sum_{ph=1}^{3} E_{APP,ph} \tag{15}$$

The calculated energies are then accumulated into buffers that store the total amount of energy consumed since the system reset. Note that these energies are different from the working variables used to accumulate energy for outputting energy pulses. There are four sets of buffers that are available: one for each phase and one for the cumulative of the phases. Within each set of buffers, the following energies are accumulated:

1. Active import energy (active energy when active energy ≥ 0)
2. Active export energy (active energy when active energy < 0)
3. Reactive Quad I energy (reactive energy when reactive energy ≥ 0 and active power ≥ 0; inductive load)
4. Reactive Quad II energy (reactive energy when reactive energy ≥ 0 and active power < 0; capacitive generator)
5. Reactive Quad III energy (reactive energy when reactive energy < 0 and active power < 0; inductive generator)
6. Reactive Quad IV energy (reactive energy when reactive energy < 0 and active power ≥ 0; capacitive load)
7. App. import energy (apparent energy when active energy ≥ 0)
8. App. export energy (apparent energy when active energy < 0)

The background process also calculates the frequency in terms of samples per mains cycle. The foreground process then converts this samples–per-mains cycle to Hertz by Equation 16:

$$\text{Frequency (Hz)} = \frac{\text{Sampling Rate (samples / second)}}{\text{Frequency (samples / cycle)}} \tag{16}$$

After the active power and apparent power have been calculated, the absolute value of the power factor is calculated. In the system's internal representation of power factor, a positive power factor corresponds to a capacitive load; a negative power factor corresponds to an inductive load. The sign of the internal representation of power factor is determined by whether the current leads or lags voltage, which is determined in the background process. Therefore, the internal representation of power factor is calculated by Equation 17:

$$\text{Internal representation of power factor} = \begin{cases} \dfrac{P_{ACT}}{P_{APPARENT}}, \text{ if capacitive load} \\ -\dfrac{P_{ACT}}{P_{APPARENT}}, \text{ if inductive load} \end{cases} \tag{17}$$

3.2.3 Background Process

The background function deals mainly with timing critical events in software. It uses the ΣΔ interrupt as a trigger to collect voltage and current samples. The ΣΔ interrupt is generated when a new voltage or current sample is ready. All voltage channels are delayed so that the voltage samples for all channels are ready at the same time. Once the voltage samples are ready and collected, sample processing is done on the voltage samples and the previous current samples. This sample processing is done by the "per_sample_dsp()" function, which also performs the necessary sensing for magnetic tamper detection. After sample processing, the background process uses the "per_sample_energy_pulse_processing()" for the calculation and output of energy-proportional pulses. Figure 12 shows the flowchart for this process.

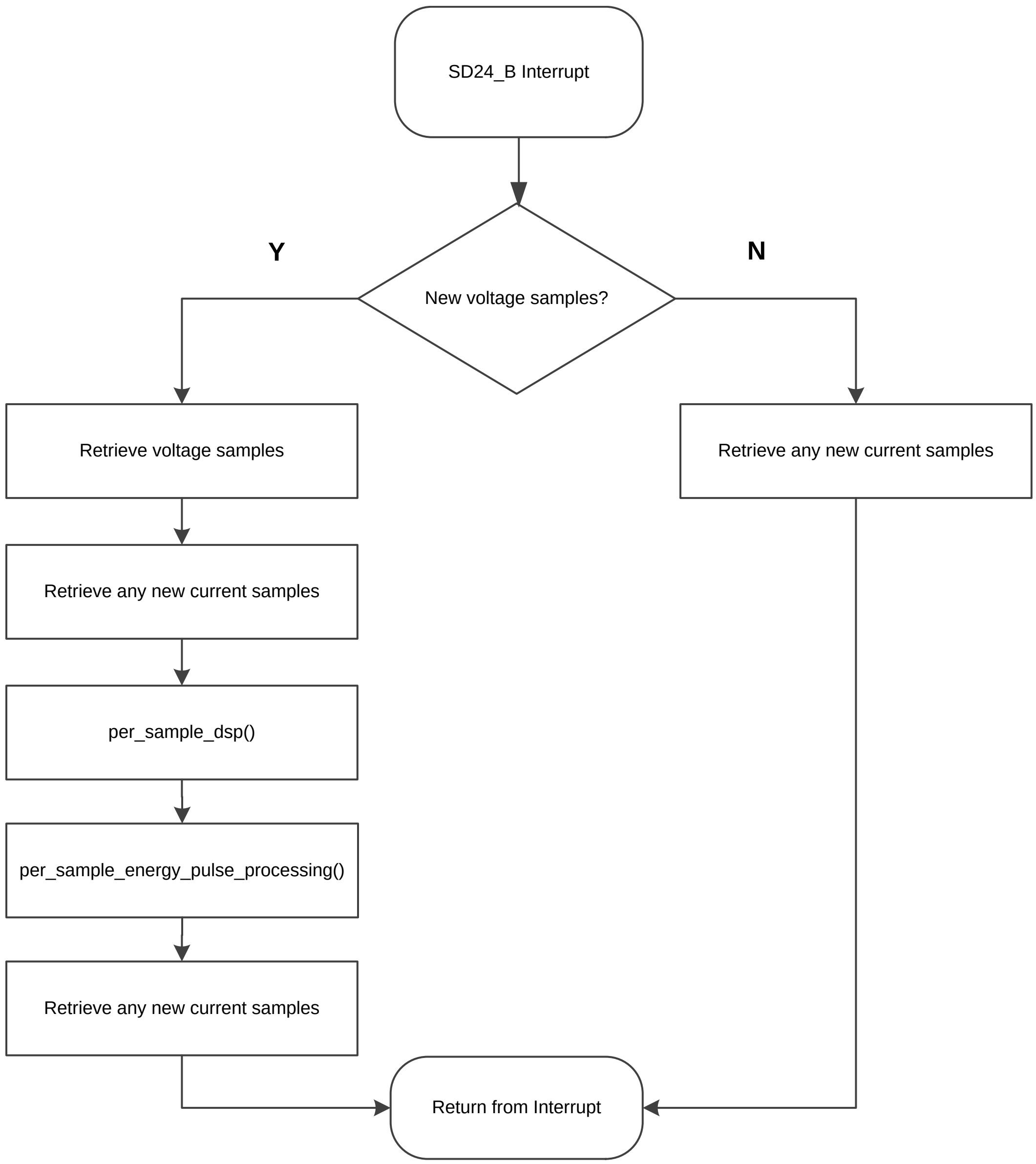

Figure 12. Background Process

3.2.3.1 per_sample_dsp()

Figure 13 shows the flowchart for the per_sample_dsp() function. The per_sample_dsp() function calculates intermediate dot product results that are fed into the foreground process for the calculation of metrology readings. Since 16-bit voltage samples are used, the voltage samples are further processed and accumulated in dedicated 48-bit registers. In contrast, because 24-bit current samples are used, the current samples are processed and accumulated in dedicated 64-bit registers. Per-phase active power and reactive power are also accumulated in 64-bit registers.

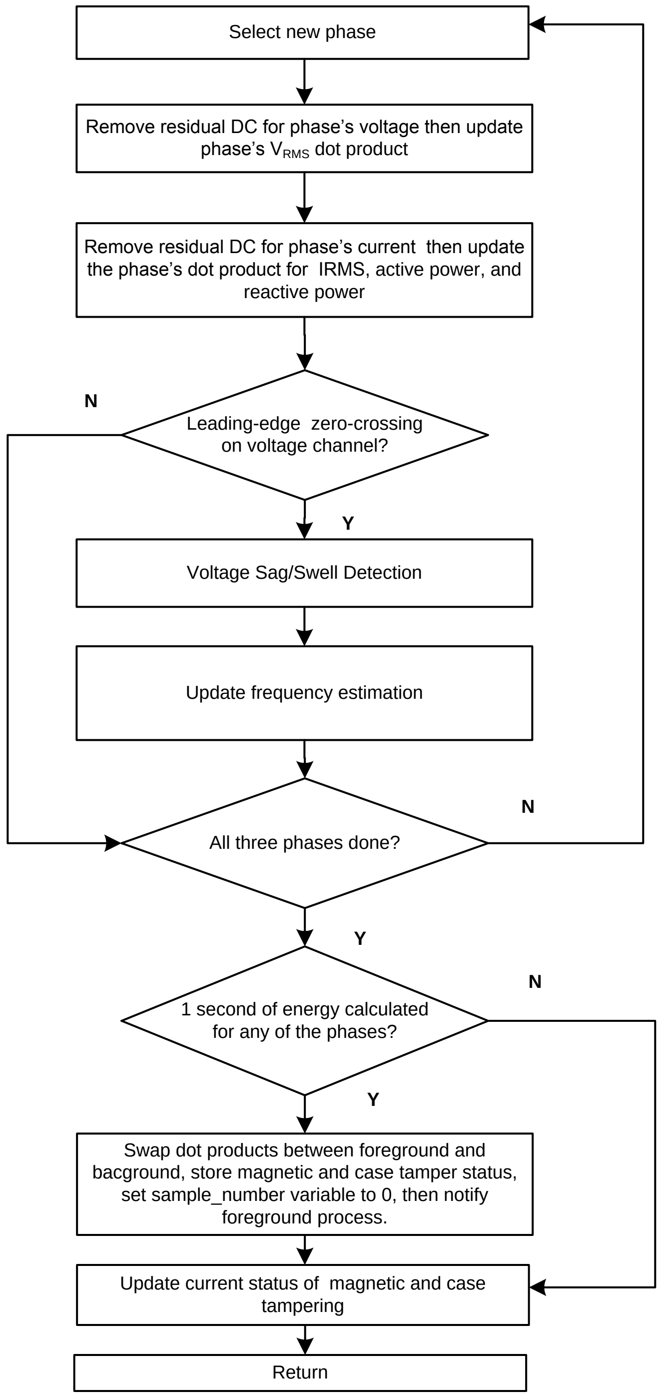

Figure 13. per_sample_dsp()

Each time the per_sample_dsp() function is called, the application checks if it is time to take a new case tampering or magnetic tampering status reading. The case tamper GPIO pin is read at a rate of 4 Hz. Similarly, each Hall sensor is read at a rate of 4 Hz with the time of sampling of each sensor distributed so that only one Hall sensor is turned ON at a time.

Also, after sufficient samples (approximately one second's worth) have been accumulated the background process triggers the foreground function to calculate the final values of V_{RMS}; I_{RMS}; active, reactive, and apparent powers; active, reactive, and apparent energy; and frequency, and power factor. In the software, there are two sets of dot products: at any given time, one is used by the foreground for calculation and the other used as the working set by the background. After the background process has sufficient samples, it swaps the two dot products so that the foreground uses the newly acquired dot products that the background process just calculated, and the background process uses a new empty set to calculate the next set of dot products. In addition, after the background process has sufficient samples it also stores the previously sensed states for magnetic and case tampering so that these states could be used in the foreground process while the background process senses the next states for magnetic and case tamper detection.

Whenever there is a leading-edge zero-crossing (− to + voltage transition) on a voltage channel, the per_sample_dsp() function is also responsible for updating the corresponding phase's frequency (in samples per cycle) and voltage sag and swell conditions. For the sag conditions, whenever the RMS voltage is below a certain user-defined threshold percentage, the number of mains cycles where this condition persists is logged as the sag duration. The number of periods in time where there was a sag condition is logged as the sag events count. Note that the sag duration corresponds to the total number of cycles in a sag condition since being reset, and is therefore not cleared for every sag event. Also, when the RMS voltage is above a certain threshold percentage, swell events and duration are logged in a similar way.

The following sections describe the various elements of electricity measurement and tamper status update in the per_sample_dsp() function.

3.2.3.1.1 Voltage and Current Signals

The output of each SD24_B digital filter is a signed integer and any stray DC or offset value on these converters are removed using a DC tracking filter. A separate DC estimate for all voltages and currents is obtained using the filter, voltage, and current samples, respectively. This estimate is then subtracted from each voltage and current sample.

The resulting instantaneous voltage and current samples generate the following intermediate results:

- Accumulated squared values of voltages and currents, which is used for V_{RMS} and I_{RMS} calculations, respectively
- Accumulated energy samples to calculate active energy
- Accumulated energy samples using current and 90° phase-shifted voltage to calculate reactive energy

The foreground process processes these accumulated values.

3.2.3.1.2 Frequency Measurement and Cycle Tracking

The instantaneous voltages are accumulated in a 48-bit register. In contrast, the instantaneous currents, active powers, and reactive powers are accumulated in 64-bit registers. A cycle tracking counter and sample counter keep track of the number of samples accumulated. When approximately one second's worth of samples have been accumulated, the background process stores these accumulation registers and notifies the foreground process to produce the average results, such as RMS and power values. Cycle boundaries trigger the foreground averaging process because this process produces very stable results.

For frequency measurements, a straight line interpolation is used between the zero crossing voltage samples. Figure 14 shows the samples near a zero cross and the process of linear interpolation.

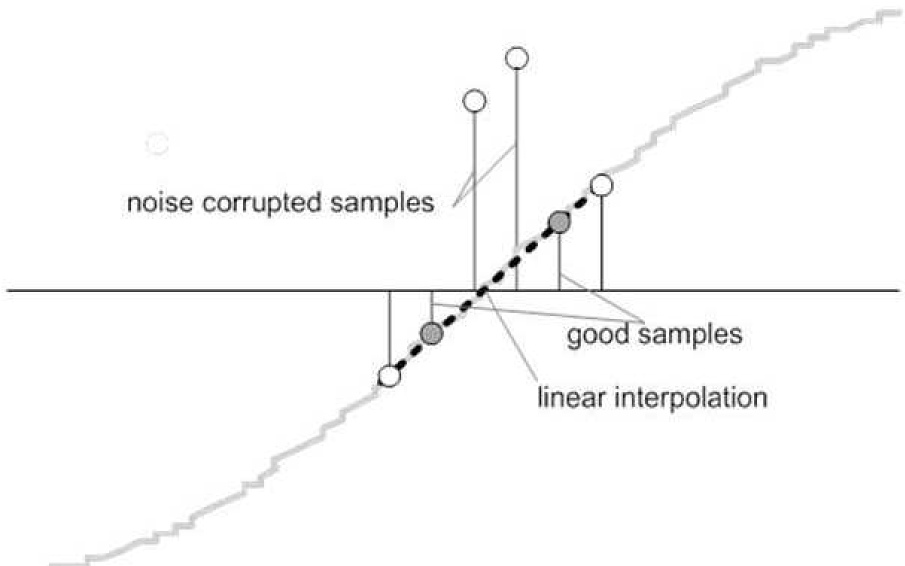

Figure 14. Frequency Measurement

Because noise spikes can also cause errors, the application uses a rate of change check to filter out the possible erroneous signals and make sure that the two points are interpolated from genuine zero crossing points. For example, with two negative samples, a noise spike can make one of the samples positive, thereby making the negative and positive pair appear as if there is a zero crossing.

The resultant cycle-to-cycle timing goes through a weak low-pass filter to further smooth out any cycle-to-cycle variations. This filtering results in a stable and accurate frequency measurement that is tolerant of noise.

3.2.3.1.3 Magnetic and Case Tampering Status Update

Each time the per_sample_dsp() function is called, the current status for magnetic and case tamper detection is updated as is shown in Figure 15. During this process, it is checked whether it is time to read the case tampering input pin or read any of the Hall sensors. All of the Hall sensors as well as the case tampering input pin are read at a rate of 4 Hz. This 4-Hz rate is achieved by reading each Hall sensor and the case tampering input pin every 1024(0x3FF) samples. Because the sample rate of the device is approximately 4096 samples per second, this results in the approximately 4 Hz sample rate for the Hall sensors and case tampering input pin. To distinguish which Hall sensors are sensing magnetic fields, only one Hall sensor is turned ON at a time. With there being approximately 1024 samples between the times a sensor is turned ON and a total of six sensors being sensed, the minimum time between when two different Hall sensors are turned ON is set equal to the floor of (1024/6), which equals 170. The actual DRV sensor that should be turned ON at a new 170 sample interval can be determined by taking the floor of (sample_number/170) then adding 1. For example, at the 850th sample, the (floor(850 / 170)) + 1 = 6th DRV sensor would be turned ON, which corresponds to U$6 on the board. The case tampering input pin is particularly sampled immediately after DRV1 is turned OFF.

The sample after a Hall sensor is turned ON, its output is read and then the sensor is turned OFF, resulting in each DRV sensor being turned ON for approximately 244 μs. Although this 244-μs time frame is longer than the minimum 50 μs needed to get a valid output (which means there would be a larger current consumption), waiting until the next sample to turn OFF the DRV5033 simplifies the timing of the duty cycling of the power. Also, this 244-μs ON time for the DRV5033 is only applicable when the device is running from main power and not when running from the backup power supply. When running from main power, the current drawn from each DRV sensor that has a 244-μs ON time is still negligible because the system will be running from mains and not a backup battery.

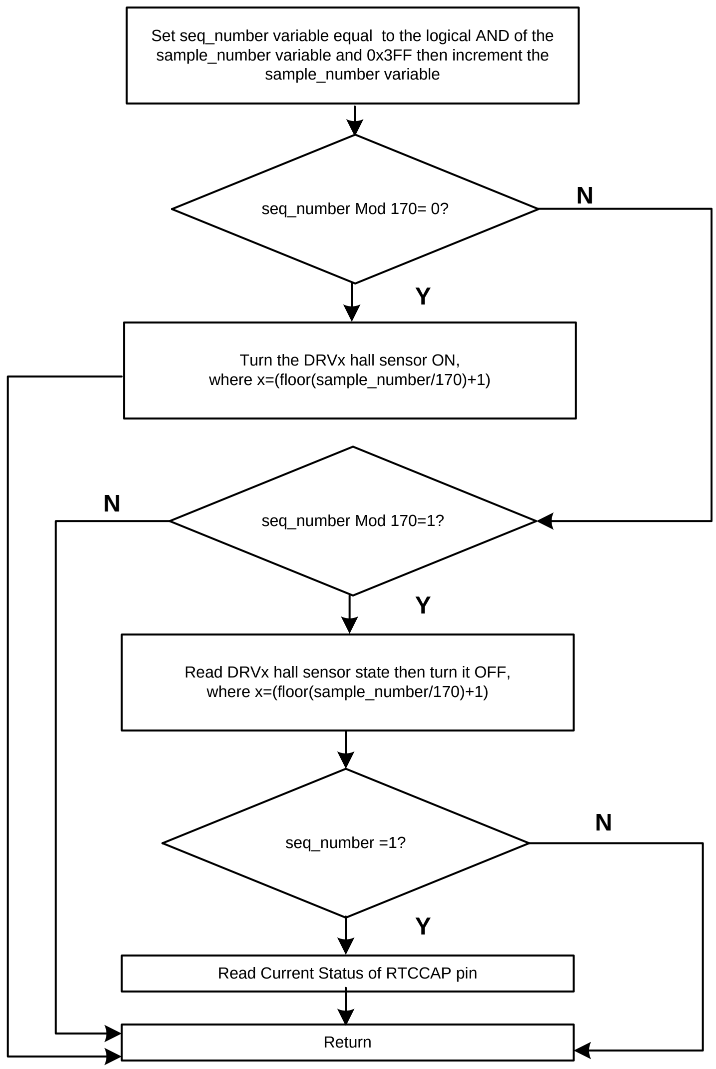

Figure 15. Magnetic and Case Tampering Status Update

3.2.3.2 LED Pulse Generation

In electricity meters, the energy consumption of the load is normally measured in a fraction of kilowatt-hour (kWh) pulses. This information can be used to accurately calibrate any meter for accuracy measurement. Typically, the measuring element (the MSP430 microcontroller) is responsible for generating pulses proportional to the energy consumed. To serve both these tasks efficiently, the pulse generation must be accurate with relatively little jitter. Although time jitters are not an indication of bad accuracy, time jitters give a negative indication of the overall accuracy of the meter. The jitter must be averaged out due to this negative indication of accuracy.

This application uses average power to generate these energy pulses. The average power (calculated by the foreground process) accumulates at every ΣΔ interrupt, thereby spreading the accumulated energy from the previous one-second timeframe evenly for each interrupt in the current one-second time frame. This accumulation process is equivalent to converting power to energy. When the accumulated energy crosses a threshold, a pulse is generated. The amount of energy above this threshold is kept and a new energy value is added on top of the threshold in the next interrupt cycle. Because the average power tends to be a stable value, this way of generating energy pulses is very steady and free of jitter.

The threshold determines the energy "tick" specified by meter manufacturers and is a constant. The tick is usually defined in pulses per kWh or just in kWh. One pulse must be generated for every energy tick. For example, in this application, the number of pulses generated per kWh is set to 6400 for active and reactive energies. The energy tick in this case is 1 kWh/6400. Energy pulses are generated and available on a header and also through LEDs on the board. GPIO pins are used to produce the pulses.

In the EVM, the LED labeled "Active" corresponds to the active energy consumption for the cumulative three-phase sum. "Reactive" corresponds to the cumulative three-phase reactive energy sum. The number of pulses per kWh and each pulse duration can be configured in software. Figure 16 shows the flow diagram for pulse generation. This flow diagram is valid for pulse generation of active and reactive energy.

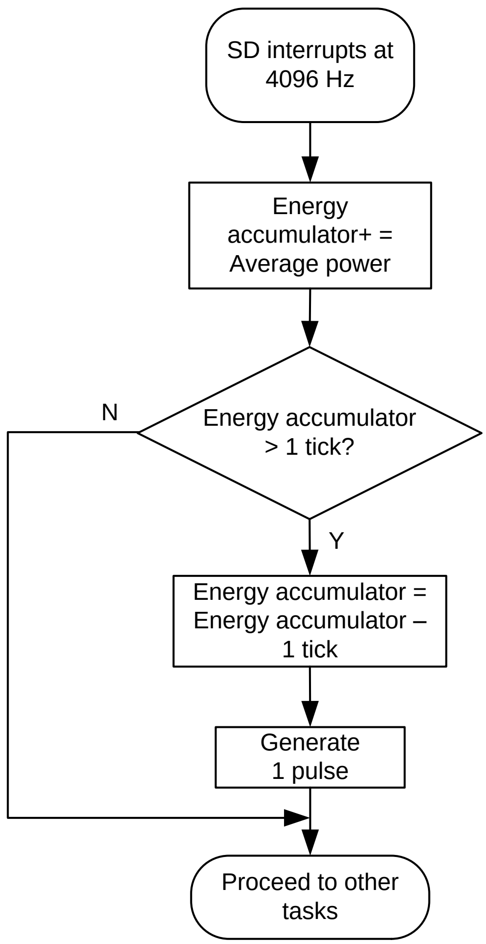

Figure 16. Pulse Generation for Energy Indication

The average power is in units of 0.001 W and a 1-kWh threshold is defined as:

$$\begin{aligned} \text{1-kWh threshold} &= 1 / 0.001 \times 1\ \text{KW} \times (\text{Number of interrupts per sec}) \times (\text{number of seconds in one hour}) \\ &= 1000000 \times 4096 \times 3600 = \text{0xD693A400000} \end{aligned} \quad (18)$$

3.2.3.3 Phase Compensation

When a CT is used as a sensor, it introduces additional phase shift on the current signals. Also, the passive components of the voltage and current input circuit may introduce another phase shift. The user must compensate the relative phase shift between voltage and current samples to ensure accurate measurements. The ΣΔ converters have programmable delay registers (ΣΔ24PREx) that can be applied to a particular channel. Using this built-in feature (PRELOAD) provides the required phase compensation. Figure 17 shows the usage of PRELOAD to delay sampling on a particular channel.

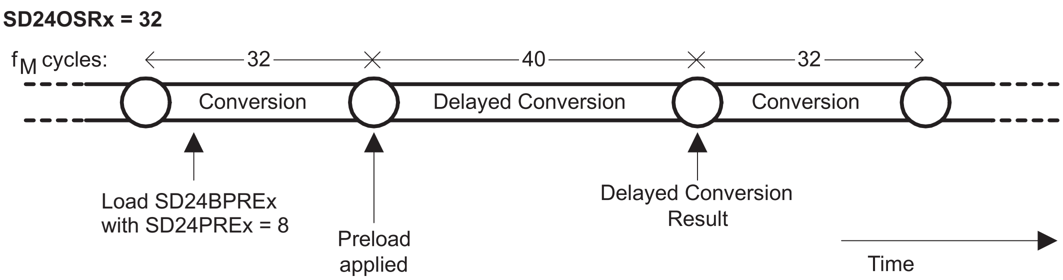

Figure 17. Phase Compensation Using PRELOAD Register

The fractional delay resolution is a function of input frequency (f_{IN}), OSR, and the sampling frequency (f_S).

$$\text{Delay resolution}_{Deg} = \frac{360^o \times f_{IN}}{OSR \times f_S} = \frac{360^o \times f_{IN}}{f_M} \tag{19}$$

In the current application, for an input frequency of 60 Hz, OSR of 256, and sampling frequency of 4096, the resolution for every bit in the preload register is about 0.02° with a maximum of 5.25° (maximum of 255 steps). When using CTs that provide a larger phase shift than this maximum, sample delays along with fractional delay must be provided.

4 Getting Started Hardware

The following figures of the EVM best describe the hardware: Figure 18 shows the top view of the system, and Figure 19 shows the location of various pieces of the system based on functionality.

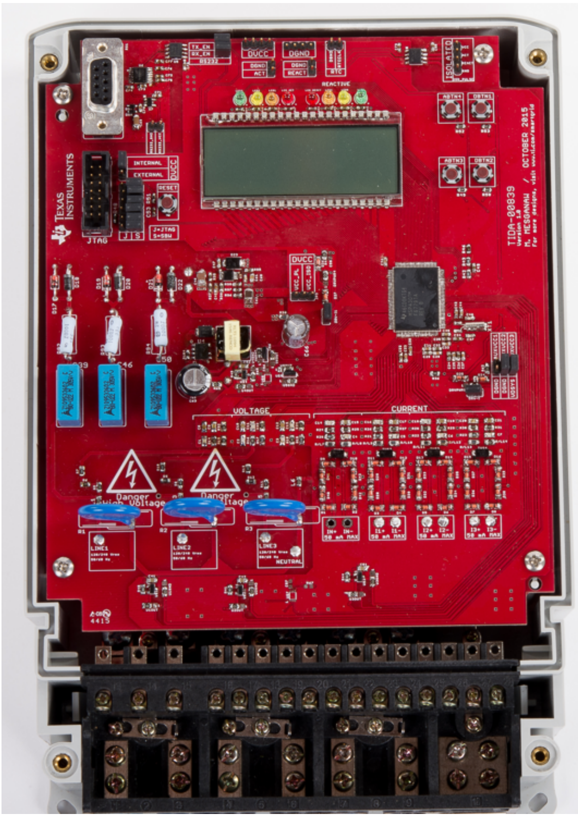

Figure 18. Top View of TIDA-00839

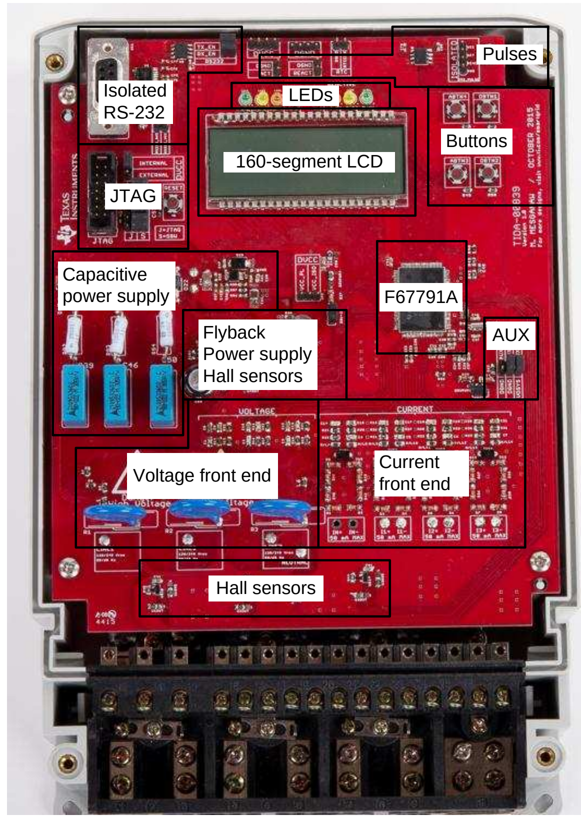

Figure 19. Top View of TIDA-00839 With Components Highlighted

4.1 Connections to the Test Setup for AC Voltages

AC voltage or currents can be applied to the board for testing purposes at these points:

- Pad "LINE_1" corresponds to the line connection for phase A.
- Pad "LINE_2" corresponds to the line connection for phase B.
- Pad "LINE_3" corresponds to the line connection for phase C.
- Pad "NEUTRAL" corresponds to the neutral voltage. The voltage between any of the three line connections to the neutral connection must not exceed 240-V AC at 50 or 60 Hz.
- I1+ and I1− are the current inputs after the sensors for phase A. When a current sensor is used, make sure that the voltage across I1+ and I1− does not exceed 930 mV. *This is currently connected to a CT on the EVM.*
- I2+ and I2− are the current inputs after the sensors for phase B. When a current sensor is used, make sure that the voltage across I2+ and I2− does not exceed 930 mV. *This is currently connected to a CT on the EVM.*
- I3+ and I3− are the current inputs after the sensors for phase C. When a current sensor is used, make sure that the voltage across I3+ and I3− does not exceed 930 mV. *This is currently connected to a CT on the EVM.*
- IN+ and IN− are the current inputs after the sensors for the neutral current. When a current sensor is used, make sure that the voltage across IN+ and IN− does not exceed 930 mV. *This is currently not connected to a CT on the EVM.*

Figure 20 and Figure 21 show the various connections that must be made to the test setup for proper functionality of the EVM. When a test AC source must be connected, the connections have to be made according to the EVM design. Figure 20 shows the connections from the top view. V_A+, V_B+, and V_C+ correspond to the line voltage for phases A, B, and C, respectively. V_N corresponds to the neutral voltage from the test AC source.

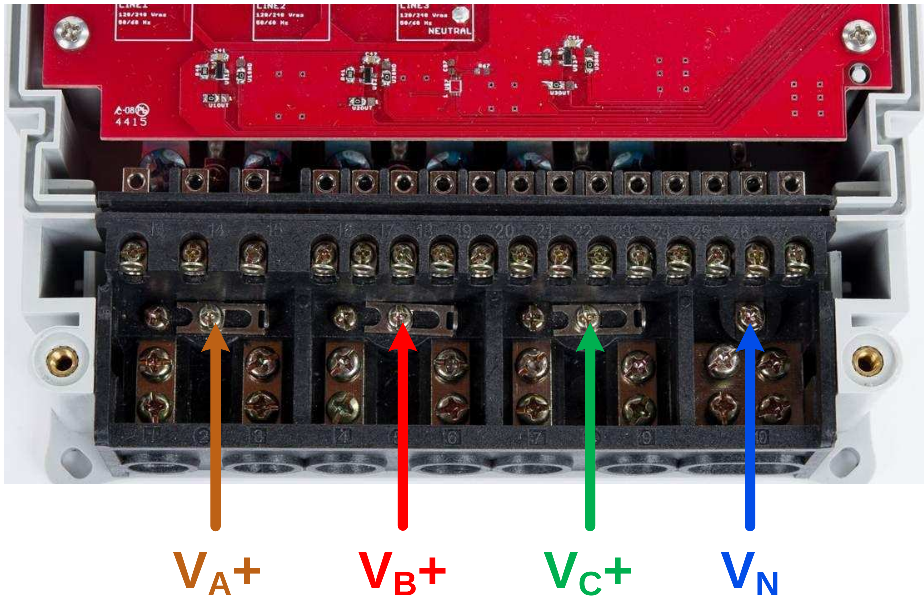

Figure 20. Top View of the EVM With Test Setup Connections

Figure 21 shows the connections from the front view. I_A+ and I_A− correspond to the current inputs for phase A; I_B+ and I_B− correspond to the current inputs for phase B; and I_C+ and I_C− correspond to the current inputs for phase C. V_N corresponds to the neutral voltage from the test setup. Note that although the EVM hardware and software supports measurement for the neutral current, the EVM obtained from Texas Instruments do not have a sensor connected to the neutral ADC channel.

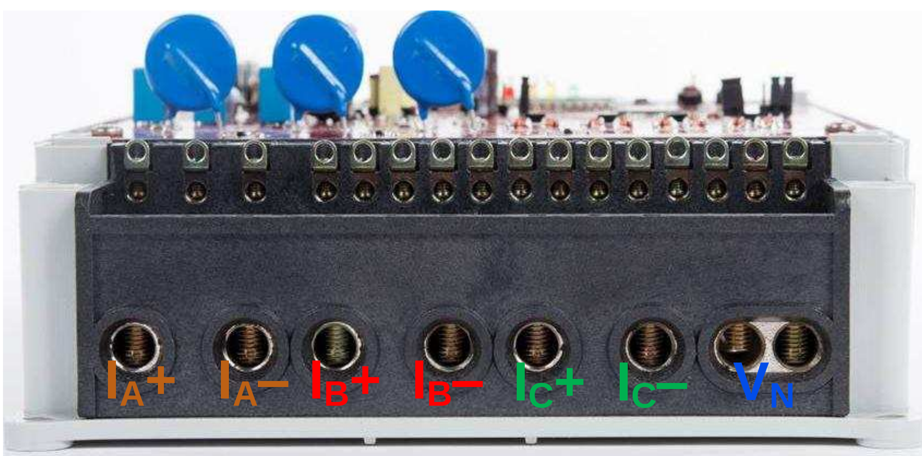

Figure 21. Front View of the EVM With Test Setup Connections

4.2 Power Supply Options and Jumper Settings

A single DC voltage rail (DVCC) powers the entire board and the UART communication. DVCC can be derived either through JTAG, external power, or the AC mains through either the capacitive power supply or flyback power supplies. Various jumper headers and jumper settings are present to add to the flexibility to the board. Some of these headers require that jumpers be placed appropriately for blocks to function correctly. Table 1 shows the functionality of each jumper on the board and the associated functionality.

Table 1. Header Names and Jumper Settings

HEADER OR HEADER OPTION NAME	TYPE	MAIN FUNCTIONALITY	VALID USE CASE	COMMENTS
ACT (Not isolated, do not probe)	2-pin header	Active energy pulses **(WARNING)**	Probe between here and ground for cumulative three-phase active energy pulses.	This header is not isolated from AC voltage, so do not connect measuring equipment unless isolators external to the EVM are available. See the ISOLATED ACT header, instead.
AUXVCC1 (Not isolated, do not probe)	2-pin header	AUXVCC1 selection and external power **(WARNING)**	Place a jumper here to connect AUXVCC1 to GND. This jumper must be present if AUXVCC1 is not used as a backup power supply. Alternatively, the header can be used to provide a backup power supply to the MSP430. To do so, connect the alternative power supply to this header.	
AUXVCC2 (Not isolated, do not probe)	2-pin jumper header	AUXVCC2 selection; AUXVCC2 external power **(WARNING)**	Place a jumper here to connect AUXVCC2 to GND. This jumper must be present if AUXVCC2 is not used as a backup power supply. Alternatively, it can be used to provide a backup power supply to the MSP430. To do so, simply connect the alternative power supply to this header. In this application, AUXVCC2 is not used so a jumper should be placed at this header.	
AUXVCC3 (Not isolated, do not probe)/JP15	2-pin jumper header	AUXVCC3 selection and external power **(WARNING)**	Place a jumper here to connect AUXVCC3 to VDSYS so that the RTC could be powered by whichever supply powers the chip. For this application, placing this jumper is necessary.	
DGND (Not isolated, do not probe)	Header	Ground voltage header **(WARNING)**	Not a jumper header, probe here for GND voltage. Connect negative terminal of bench or external power supply when powering the board externally.	Do not probe if board is powered from AC mains, unless the AC mains are isolated. This voltage can be hot or neutral if AC wall plug is connected to the system.
DRV-I	2-pin jumper header	U$1, U$2, U$3 Enable/disable and current consumption measurement pin **(WARNING)**	This header can be used to disable the set of Hall sensors near the current transformers(U$1, U$2, and U$3). To enable these Hall sensors, place a jumper here. In addition, this header can be used for taking the average current consumption readings for this set of Hall sensors.	Do not probe if board is powered from AC mains, unless the AC mains are isolated. This voltage can be hot or neutral if AC wall plug is connected to the system. Please note that whenever the Hall sensors are disabled by not placing a jumper here the corresponding Hall sensor LEDs would remain ON.
DRV-I1	2-pin jumper header	U$4, U$5, U$6 Enable/disable and current consumption measurement pin **(WARNING)**	This header can be used to disable the set of Hall sensors near the current transformers (U$4, U$5, and U$6). To enable these Hall sensors, place a jumper here. In addition, this header can be used for taking the average current consumption readings for this set of Hall sensors.	Do not probe if board is powered from AC mains, unless the AC mains are isolated. This voltage can be hot or neutral if AC wall plug is connected to the system. Please note that whenever the Hall sensors are disabled by not placing a jumper here the corresponding Hall sensor LEDs would remain ON.

Table 1. Header Names and Jumper Settings (continued)

HEADER OR HEADER OPTION NAME	TYPE	MAIN FUNCTIONALITY	VALID USE CASE	COMMENTS
DRVPWR1	3-pad jumper resistor footprint	Selection for U$1, U$2, U$3 power source	Place a 0-Ω resistor between the center pad and pad 1 so that U$1, U$2, and U$3 are powered from AUXVCC1 and DVCC using external diodes to switch between the supplies. Place a 0-Ω resistor between the center pad and pad 3 to power U$1, U$2, and U$3 from AUXVCC1 and DVCC using the internal switching mechanism of the MSP430F67791A's AUX module. In this application, the 0-Ω resistor should be placed between the center pad and pad 3.	All three pads should not be shorted together.
DRVPWR4	3-pad jumper resistor footprint	Selection for U$4, U$5, U$6 power source	Place a 0-Ω resistor between the center pad and pad 1 so that U$4, U$5, and U$6 are powered from AUXVCC1 and DVCC using external diodes to switch between the supplies. Place a 0-Ω resistor between the center pad and pad 3 to power U$1, U$2, and U$3 from AUXVCC1 and DVCC using the internal switching mechanism of the MSP430F67791A's AUX module. In this application, the 0-Ω resistor should be placed between the center pad and pad 3.	All three pads should not be shorted together.
DVCC (Not isolated, do not probe)	Header	VCC voltage header **(WARNING)**	Not a jumper header; probe here for VCC voltage. Connect positive terminal of bench or external power supply when powering the board externally.	Do not probe if board is powered from AC mains, unless the AC mains are isolated.
DVCC EXTERNAL (Do not connect JTAG if AC mains is the power source ;isolated JTAG or supply is fine)	Jumper header option	JTAG external power selection option **(WARNING)**	Place a jumper at this header option to select external voltage for JTAG programming.	This jumper option and the DVCC INTERNAL jumper option comprise one three-pin header used to select the voltage source for JTAG programming.
DVCC INTERNAL (Do not connect JTAG if AC mains is the power source)	Jumper header option	JTAG internal power selection option **(WARNING)**	Place a jumper at this header option to power the board using JTAG and to select the voltage from the USB FET for JTAG programming.	This jumper option and the DVCC EXTERNAL jumper option comprise one three-pin header used to select the voltage source for JTAG programming.
DVCC VCC_ISO	Jumper header option	Flyback power supply select **(WARNING)**	Place a jumper at this header position to power the board through AC mains using the flyback power supply.	Place a jumper only if AC mains voltage is required to power the DVCC rail. This header option and the DVCC VCC_PL header option comprise one three-pin header that can be used to select either the capacitive power supply, flyback power supply, or neither (if jumper not present).

Table 1. Header Names and Jumper Settings (continued)

HEADER OR HEADER OPTION NAME	TYPE	MAIN FUNCTIONALITY	VALID USE CASE	COMMENTS
DVCC VCC_PL (Not isolated, do not probe)	Jumper header option	Capacitor power supply select **(WARNING)**	Place a jumper at this header position to power the board through AC mains using the capacitor power supply.	Place a jumper only if AC mains voltage is required to power the DVCC rail. Do not debug using JTAG unless AC source is isolated or JTAG is isolated. This header option and the DVCC VCC_ISO header option comprise one three-pin header that selects a capacitive power supply, a flyback power supply, or neither.
ISO_ACT	1-pin header	Isolated active energy pulses	Probe between here and ground for cumulative three-phase active energy pulses	This header is isolated from AC voltage so it is safe to connect to scope or other measuring equipment since isolators are already present. However, either 3.3 or 5 V should be applied between ISO_GND and ISO_VCC in order to produce pulses on this pin. The pulses would have a logical high voltage that is equal to the voltage applied between ISO_GND and ISO_VCC.
ISO_GND	1-pin header	Isolated ground for energy pulses	Ground connection for the isolated active and reactive energy pulses.	This header is Isolated from AC voltage so it is safe to connect to scope or other measuring equipment since isolators are already present. However, either 3.3 or 5 V should be applied between ISO_GND and ISO_VCC in order to produce pulses on this pin. The pulses would have a logical high voltage that is equal to the voltage applied between ISO_GND and ISO_VCC.
ISO_REACT	1-pin header	Isolate reactive energy pulses	Probe between here and ground for cumulative three-phase reactive energy pulses	This header is isolated from AC voltage so it is safe to connect to scope or other measuring equipment since isolators are already present. However, either 3.3 or 5 V should be applied between ISO_GND and ISO_VCC in order to produce pulses on this pin. The pulses would have a logical high voltage that is equal to the voltage applied between ISO_GND and ISO_VCC.
ISO_VCC	1-pin header	Isolated VCC for energy pulses	VCC connection for the isolated active and reactive energy pulses.	Either 3.3 or 5 V should be applied between ISO_GND and ISO_VCC in order to produce isolated active and reactive pulses on the respective isolated ISO_ACT and ISO_REACT pins. The pulses would have a logical high voltage that is equal to the voltage applied between ISO_GND and ISO_VCC.
J (Do not connect JTAG if AC mains is the power source)	Jumper header option	4-wire JTAG programming option **(WARNING)**	Place jumpers at the J-header options of all of the six JTAG communication headers to select 4-wire JTAG.	

Table 1. Header Names and Jumper Settings (continued)

HEADER OR HEADER OPTION NAME	TYPE	MAIN FUNCTIONALITY	VALID USE CASE	COMMENTS
REACT (Not isolated, do not probe)	1-pin header	Reactive energy pulses **(WARNING)**	Not a jumper header, probe between here and ground for cumulative three-phase reactive energy pulses.	Place jumpers at the six headers to select a JTAG communication option. Each of these six headers have a J option and an S option to select either 4-wire JTAG or SBW. To enable 4-wire JTAG, configure all of these headers for the J option. To enable SBW, configure all of the headers for the S option.
RS232_GND	1-pin header	Ground connection for the isolated RS-232	Ground connection for the isolated RS-232 circuitry.	
RS232_3.3	1-pin header	Voltage source harvested from RS-232 line	Voltage source that is used to power the TRS3232 and ISO7321 for isolated RS-232 communication. This voltage source is harvested from the RS-232 line.	
RTCCLK (Not isolated, do not probe)	2-pin header	RTC calibration **(WARNING)**	Probe here to measure the frequency of RTCCLK, which is used for calibrating the RTC.	
RX_EN	Jumper header	RS-232 receive enable	Place a jumper here to enable receiving characters using RS-232.	
S (Do not connect JTAG if AC mains is the power source)	Jumper header option	SBW JTAG programming option **(WARNING)**	Place jumpers at the S-header options of all of the six JTAG communication headers to select SBW.	
TX_EN	Jumper header	RS-232 transmit enable	Place a jumper here to enable RS-232 transmissions.	
UxOUT (where x is between 1 to 6)	3-pad jumper resistor footprint	Connection selection for the U$x Hall sensor's output pin	Place a 0-Ω resistor between the center pad and pad 1 so that U$x's output is connected to a GPIO pin that is not shared by other Hall sensors. Place a 0-Ω resistor between the center pad and pad 3 to connect U$x's output pin to the GPIO pin that is shared with the other two Hall sensors within that set. In this application, the 0-Ω resistor should be placed between the center pad and pad 3.	All three pads should not be shorted together.
UxGND (where x is between 1 to 6)	3-pad jumper resistor footprint	Connection selection for the U$x Hall sensor's ground pin	Place a 0-Ω resistor between the center pad and pad 1 to connect U$x to ground. Place a 0-Ω resistor between the center pad and pad 3 to connect U$x to a GPIO pin so that the power to the device could be duty cycled. In this application, the 0-Ω resistor should be placed between the center pad and pad 3.	All three pads should not be shorted together.

4.3 LEDS and Buttons

Table 2. Button Functionality

BUTTON NAME	DESCRIPTION
ABTN3	ABTN3 simulates a case tampering event. The first time this button is pressed is logged and later displayed on the LCD. The LCD also displays the current status of whether this button is still pressed or not.
ABT4	Not used
DBTN1	Pressing this button clears the first magnetic tampering event so that the next time magnetic tampering occurs is logged as the "first" magnetic tamper event.
DBTN2	Pressing this button clears the first case tampering event so that the next time ABTN3 is pressed this time is logged as the "first" case tamper event.

Table 3. LED Functionality

LED NAME	DESCRIPTION
LED1	Whenever the chip is being powered from DVCC, LED1 represents the current state of magnetic sensing on U$1. When this LED is ON, magnetic tampering has been detected from the U$1 Hall sensor, which is in the set of Hall sensors near the current transformers.
LED2	Whenever the chip is being powered from DVCC, LED2 represents the current state of magnetic sensing on U$2. When this LED is ON, magnetic tampering has been detected from the U$2 Hall sensor, which is in the set of Hall sensors near the current transformers.
LED3	Whenever the chip is being powered from DVCC, LED3 represents the current state of magnetic sensing on U$3. When this LED is ON, magnetic tampering has been detected from the U$3 Hall sensor, which is in the set of Hall sensors near the current transformers.
LED4	Whenever the chip is being powered from DVCC, LED4 represents the current state of magnetic sensing on U$4. When this LED is ON, magnetic tampering has been detected from the U$4 Hall sensor, which is in the set of Hall sensors near the flyback power supply transformer.
LED5	Whenever the chip is being powered from DVCC, LED5 represents the current state of magnetic sensing on U$5. When this LED is ON, magnetic tampering has been detected from the U$5 Hall sensor, which is in the set of Hall sensors near the flyback power supply transformer.
LED6	Whenever the chip is being powered from DVCC, LED6 represents the current state of magnetic sensing on U$6. When this LED is ON, magnetic tampering has been detected from the U$6 Hall sensor, which is in the set of Hall sensors near the flyback power supply transformer.
LED_ACT	This LED corresponds to the cumulative active energy consumption.
LED_REACT	This LED corresponds to the cumulative reactive energy consumption.

5 Getting Started Firmware

The source code is developed in the IAR™ environment using the IAR Embedded Workbench® Integrated Development Environment (IDE) version 6.10.1 for the MSP430 IDE and version 7.0.5.3137 for IAR common components. Earlier versions of IAR cannot open the project files. When the project is loaded in IAR version 6.x or later, the IDE may prompt the user to create a backup. Click "YES" to proceed. The energy metrology software has three main parts:

- The toolkit that contains a library of mostly mathematics routines
- The metrology code that is used for calculating metrology parameters
- The application code that is used for the host-processor functionality of the system (communication, LCD, RTC setup, and so forth)

Figure 22 shows the contents of the source folder.

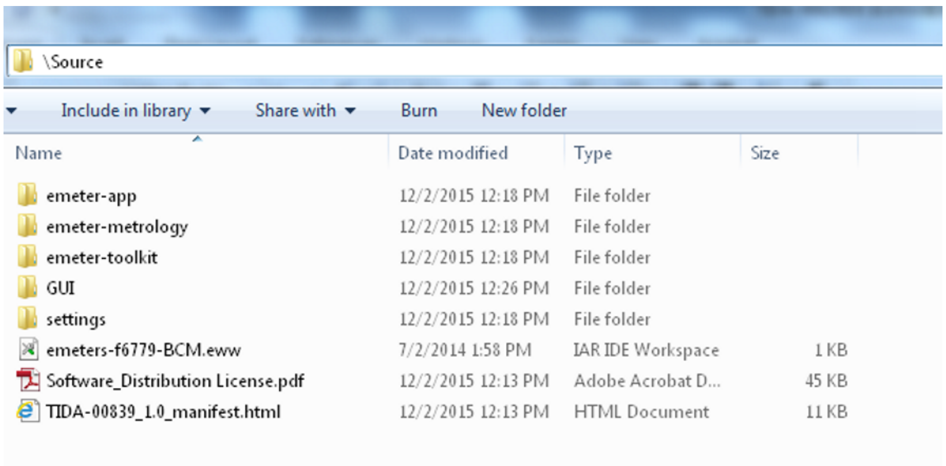

Figure 22. Source Folder Structure

Within the emeter-app-6779 folder in the emeter-app folder, the emeter-app-6779.ewp project corresponds to the application code. Similarly, within the emeter-metrology-6779 folder in the emeter-metrology folder, the emeter-metrology-6779.ewp project corresponds to the portion of the code for metrology. Additionally, the folder emeter-toolkit-6779 within the emeter-toolkit has the corresponding toolkit project file emeter-toolkit-6779.ewp. For first-time use, TI recommends to rebuild all three projects by performing the following steps:

1. Open the IAR IDE.
2. Open the F6779 workspace, which is located in the Source folder.
3. Within IARs workspace window, click the Overview tab to have a list view of all the projects.
4. Right-click the emeter-toolkit-6779 option in the workspace window and select "Rebuild All", as Figure 22 shows.
5. Right-click the emeter-metrology-6779 option in the workspace window and select "Rebuild All", as Figure 23 shows.
6. Within IARs workspace window, click the emeter-app-6779 tab.
7. Within the workspace window, select emeter-app-6779, click Rebuild All as Figure 24 shows, and then download this project onto the MSP430F67791A.

NOTE: If any changes are made to any of the files in the toolkit project and the project is compiled, the metrology project must be recompiled. After recompiling the metrology project, the application project must then be recompiled. Similarly, if any changes are made to any of the files in the metrology project and the project is compiled, the application project must then be recompiled.

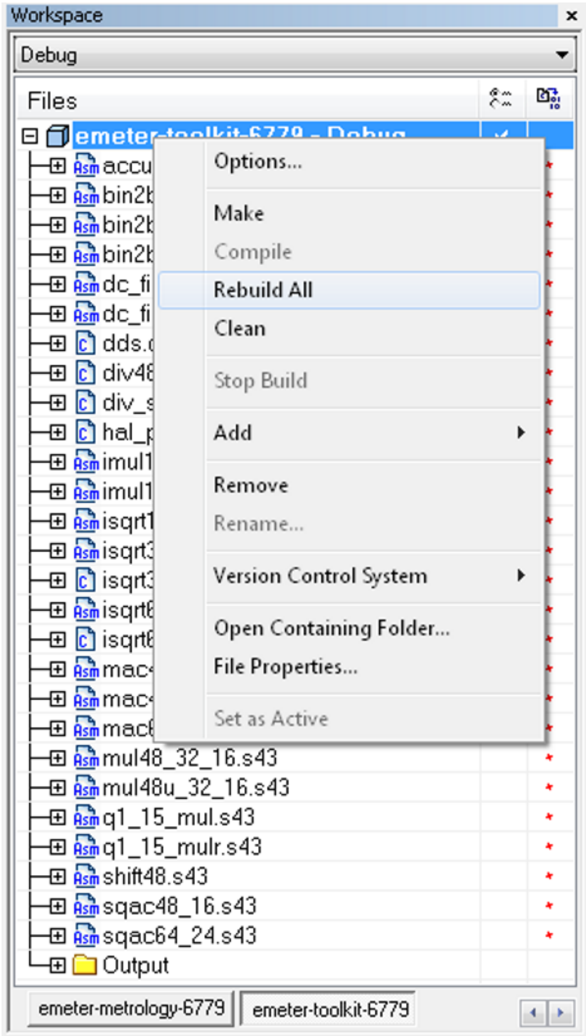

Figure 23. Toolkit Project Compilation

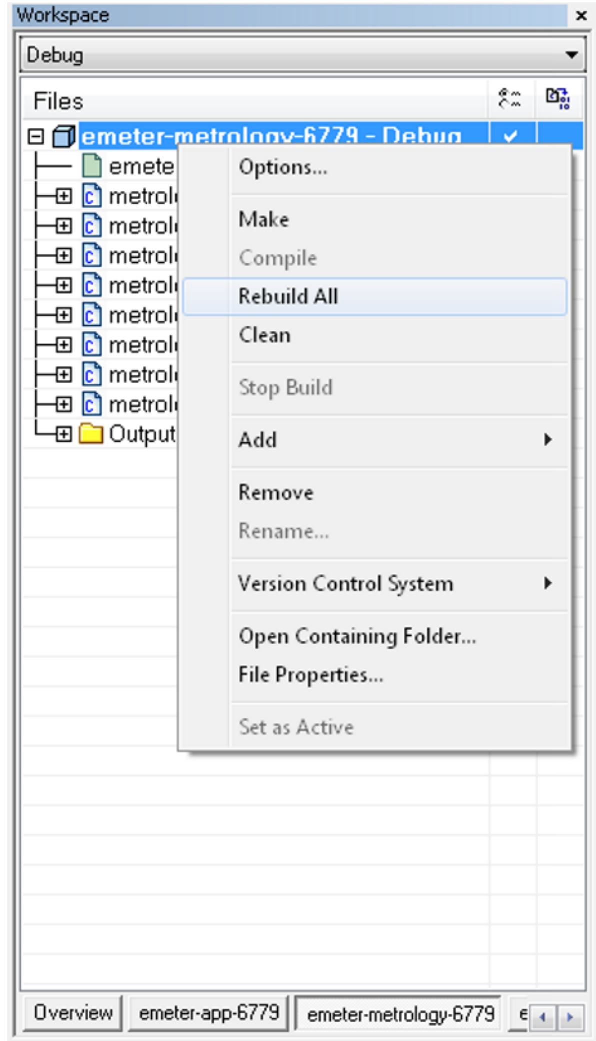

Figure 24. Metrology Project Compilation

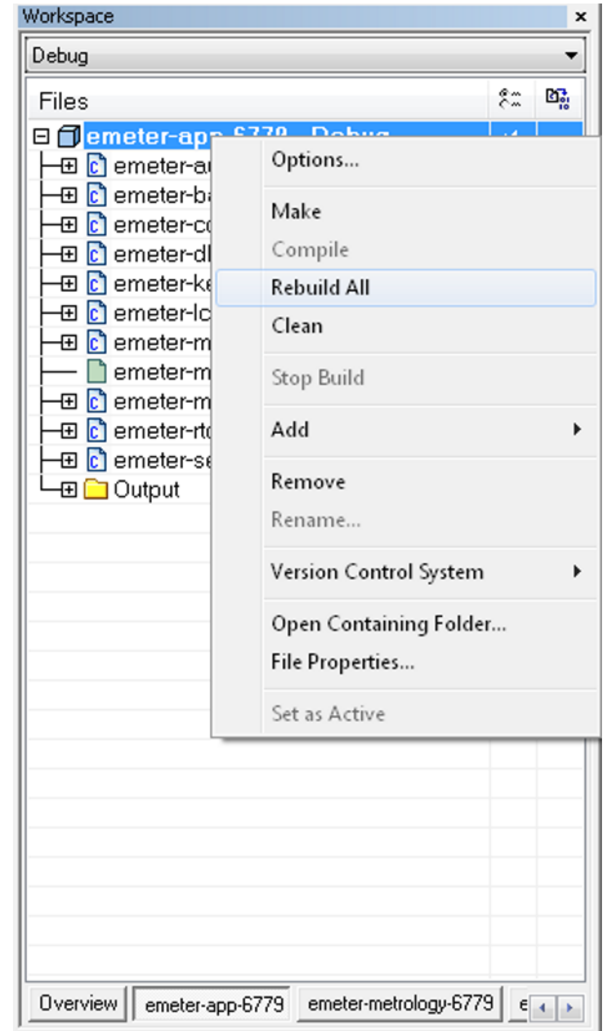

Figure 25. Application Project Compilation

6 Test Setup

6.1 Metrology Test Setup

For performing metrology testing, a source generator was used to provide the voltages and currents to the board at the proper locations (see Section 4.1). The design tests used a nominal voltage of 230 V, calibration current of 10 A, and nominal frequency of 50 Hz. In the tests, current is varied from 50 mA to 100 A. For each current, a phase shift of 0°, 60°, and −60° is applied between the voltage and current.

When voltage and current are applied to the system, the board outputs active energy pulses at a rate of 6400 pulses/kWh. This pulse output feeds into a reference meter that determines the active energy % error (for the equipment used in this test, the reference meter was integrated in the same equipment used for the source generator). The active energy % error is based on the actual energy provided to the board and the measured energy as determined by the active energy output pulse of the system. Based on this energy pulse measurement, a plot of active energy % error versus current is created for 0°, 60, and −60° phase shifts, as Section 8.1 shows. A similar method is used to calculate the reactive energy error.

To test the magnetic penalty functionality, 230 V and 10 A are first applied to the system. Subsequently, a 1-Tesla magnet is applied close to the system near the CTs. After applying the magnet and observing the corresponding magnetic tampering LEDs turn ON, the displayed current is verified to be set equal to the penalty current (100 A by default).

6.2 Current Consumption Test Setup

Because the power to each DRV5033 sensors is duty cycled, using a multimeter to measure the current consumption will not provide accurate readings for the average current. As a result, the current consumption of a set of DRV sensors is tested by estimating the average of the voltage across a resistor with known resistance. Specifically, the jumper at DRV-I1 is removed and each end of a resistor is connected to a different pin of the 2-pin DRV-I1 header. Current consumption readings are taken for the cases where the MSP430F67791A is powered from DVCC and AUXVCC1 because these two cases have different duty cycling schemes and durations. A 49-Ω resistor is connected across DRV-I1 for the case DVCC is powering the chip and a 10-Ω resistor is used for the case the chip is powered from AUXVCC1. The lower resistance for the AUXVCC1 case is due to the peak current being higher for this case because all Hall sensors will be turned ON at the same time compared to the DVCC case where only one sensor is ON at a time. In addition, the current consumption is estimated both for when a magnetic tamper event is currently being detected and when it is not currently being detected.

Once the resistor is connected to DRV-I1, an oscilloscope is connected to the ends of the resistor. The waveform on the oscilloscope is then divided into regions that together cover one period of the waveform. The duration of each region and the associated peak voltage for that region is logged. The peak voltage is converted to peak current by dividing by the peak voltage by the known resistance value of the resistor across DRV_I1. Using the different peak currents and durations, an upper-bound of the average current is calculated by the following formula:

$$I_{Avg,bound} \leq \frac{\sum_{n=1}^{\text{Region count}} I_{peak,n} \times t_n}{\sum_{n=1}^{\text{Region count}} t_n} \tag{20}$$

Since DRV-I1 powers three Hall sensors, this calculated upper bound for average current corresponds to the current consumption of all three sensors. To calculate the per sensor consumption, the calculated upper bound for average current is then divided by 3.

7 Viewing Metrology Readings and Calibration

The values of the metrology parameters can be viewed on the LCD or the GUI.

7.1 Viewing Results Through LCD

The LCD scrolls between parameter values approximately every two seconds. The set of parameters displayed on the LCD depends on whether the chip is powered from DVCC or AUXVCC1. For each parameter that shows on the LCD, three items always display on the screen: a symbol used to denote the phase of the parameter, a text and symbol combination to denote the parameter that is being displayed, and the actual value of the parameter. In addition to the three items always displayed, special characters will be displayed on the LCD whenever magnetic tampering is currently being detected, the case is currently opened, and the device is powered from AUXVCC1. See Figure 26 to Figure 28 for the symbols corresponding to these statuses.

Figure 26. Symbol for Indicating Magnetic Tampering is Currently Detected

Figure 27. Symbol for Case Being Opened

Figure 28. Symbol for the MSP430F67791A Being Powered from AUXVCC1

The phase symbol is displayed at the top of the LCD and denoted by a triangle shape. The orientation of the symbol determines the corresponding phase. Figure 29, Figure 30, and Figure 31 show the mapping between the different orientations of the triangle and the phase descriptor:

Figure 29. Symbol for Phase A

Figure 30. Symbol for Phase B

Figure 31. Symbol for Phase C

Aggregate results (such as cumulative active and reactive power) and parameters that are independent of phase (such as current time and date) are denoted by clearing all of the phase symbols on the LCD.

The bottom line of the LCD is used to denote the value of the parameter being displayed. The text to denote the parameter being shown displays on the top line of the LCD. Table 4 shows the different metering parameters that are displayed on the LCD and the associated units in which they are displayed. The **DESIGNATION** column shows which characters correspond to which metering parameter.

Table 4. Displayed Parameters

PARAMETER	DESIGNATION	UNITS	COMMENTS
Active power	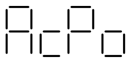	Watts (W)	This parameter displays for each phase. The aggregate active power is also displayed. This is only displayed on the LCD when the chip is being powered from DVCC.
Reactive power		Volt-Ampere Reactive (VAR)	This parameter displays for each phase. The aggregate reactive power is also displayed. This is only displayed on the LCD when the chip is being powered from DVCC.
Apparent power		Volt-Ampere (VA)	This parameter displays for each phase. This is only displayed on the LCD when the chip is being powered from DVCC.
Power factor		Constant between 0 and 1	This parameter displays for each phase. This is only displayed on the LCD when the chip is being powered from DVCC.
Voltage		Volts (V)	This parameter displays for each phase. This is only displayed on the LCD when the chip is being powered from DVCC.
Current	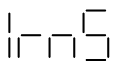	Amps (A)	This parameter displays for each phase. This is only displayed on the LCD when the chip is being powered from DVCC.
Frequency	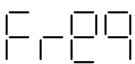	Hertz (Hz)	This parameter displays for each phase. This is only displayed on the LCD when the chip is being powered from DVCC.
Total consumed active energy	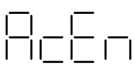	kWh	This parameter displays for each phase. This is only displayed on the LCD when the chip is being powered from DVCC.
Total consumed reactive energy		kV_{ARH}	This parameter displays when the sequence of aggregate readings are displayed. This displays the sum of the reactive energy in quadrant 1 and quadrant 4. This is only displayed on the LCD when the chip is being powered from DVCC.
Current time	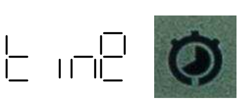	Hour:minute:second	When the MSP430F67791A is powered from DVCC, this parameter displays when the sequence of aggregate readings are displayed. This parameter is not displayed once per phase. To distinguish between displaying the current time, the time of the first magnetic event, and the time of the first case event, the timer icon is displayed on the LCD.
Current date		Year:month:day	When the MSP430F67791A is powered from DVCC, this parameter displays when the sequence of aggregate readings are displayed. This parameter is not displayed once per phase. To distinguish between displaying the current date, the date of the first magnetic event, and the date of the first case event, the timer icon is displayed on the LCD.
Time of first magnetic tamper event	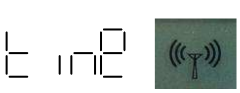	Hour:minute:second	When the MSP430F67791A is powered from DVCC, this parameter displays when the sequence of aggregate readings are displayed. This parameter is not displayed once per phase. To distinguish between displaying the current time, the time of the first magnetic event, and the time of the first case event, the antennae icon is displayed on the LCD. In the case a magnetic tamper event has not occurred, the LCD displays "None" for this parameter.

Table 4. Displayed Parameters (continued)

PARAMETER	DESIGNATION	UNITS	COMMENTS
Time of first magnetic tamper event	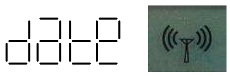	Year:month:day	When the MSP430F67791A is powered from DVCC, this parameter displays when the sequence of aggregate readings are displayed. This parameter is not displayed once per phase. To distinguish between displaying the current date, the date of the first magnetic event, and the date of the first case event, the antennae icon is displayed on the LCD. In the case a magnetic tamper event has not occurred, the LCD displays "None" for this parameter.
Time of first case tamper event	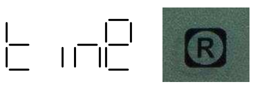	Hour:minute:second	When the MSP430F67791A is powered from DVCC, this parameter displays when the sequence of aggregate readings are displayed. This parameter is not displayed once per phase. To distinguish between displaying the current time, the time of the first magnetic event, and the time of the first case event, the boxed-R icon is displayed on the LCD. In the case a case tamper event has not occurred, the LCD displays "None" for this parameter.
Time of first case tamper event	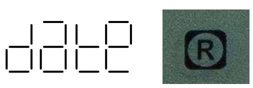	Year:month:day	When the MSP430F67791A is powered from DVCC, this parameter displays when the sequence of aggregate readings are displayed. This parameter is not displayed once per phase. To distinguish between displaying the current date, the date of the first magnetic event, and the date of the first case event, the boxed-R icon is displayed on the LCD. In the case a magnetic tamper event has not occurred, the LCD displays "None" for this parameter.

Figure 32 shows an example of phase B's measured power factor of 1 displayed on the LCD when the case is open and magnetic tampering being currently detected.

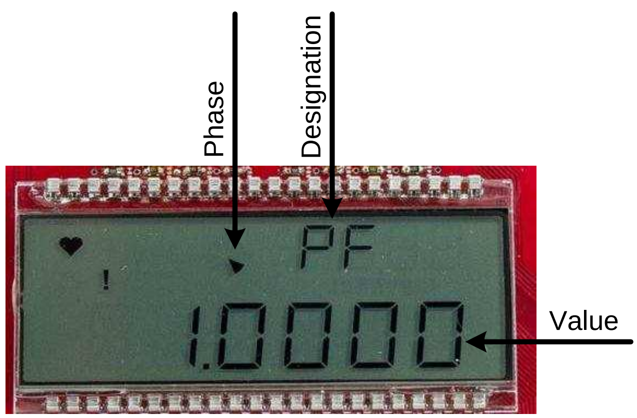

Figure 32. LCD

7.2 Calibrating and Viewing Results Through PC

7.2.1 Viewing Results

To view the metrology parameter values from the GUI, perform the following steps:

1. Connect the EVM to a PC using an RS-232 cable.
2. Open the GUI folder and open calibration-config.xml in a text editor.
3. Change the port name field within the meter tag to the COM port connected to the system. As Figure 33 shows, this field is changed to COM7.

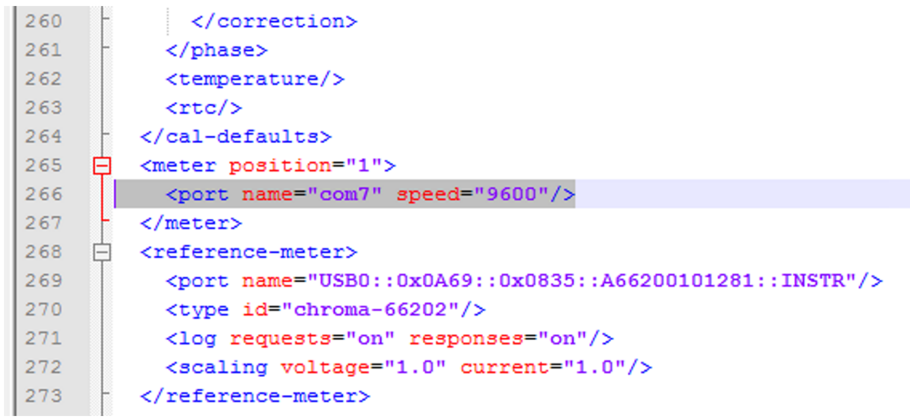

```
      </correction>
    </phase>
    <temperature/>
    <rtc/>
  </cal-defaults>
  <meter position="1">
    <port name="com7" speed="9600"/>
  </meter>
  <reference-meter>
    <port name="USB0::0x0A69::0x0835::A66200101281::INSTR"/>
    <type id="chroma-66202"/>
    <log requests="on" responses="on"/>
    <scaling voltage="1.0" current="1.0"/>
  </reference-meter>
```

Figure 33. GUI Config File Changed to Communicate With Energy Measurement System

4. Run the calibrator.exe file, which is located in the GUI folder. If the COM port in the calibration-config.xml was changed in the previous step to the COM port connected to the EVM, the GUI opens (see Figure 34). If the GUI connects properly to the EVM, the top-left button is green. If there are problems with connections or if the code is not configured correctly, the button is red. Click the green button to view the results.

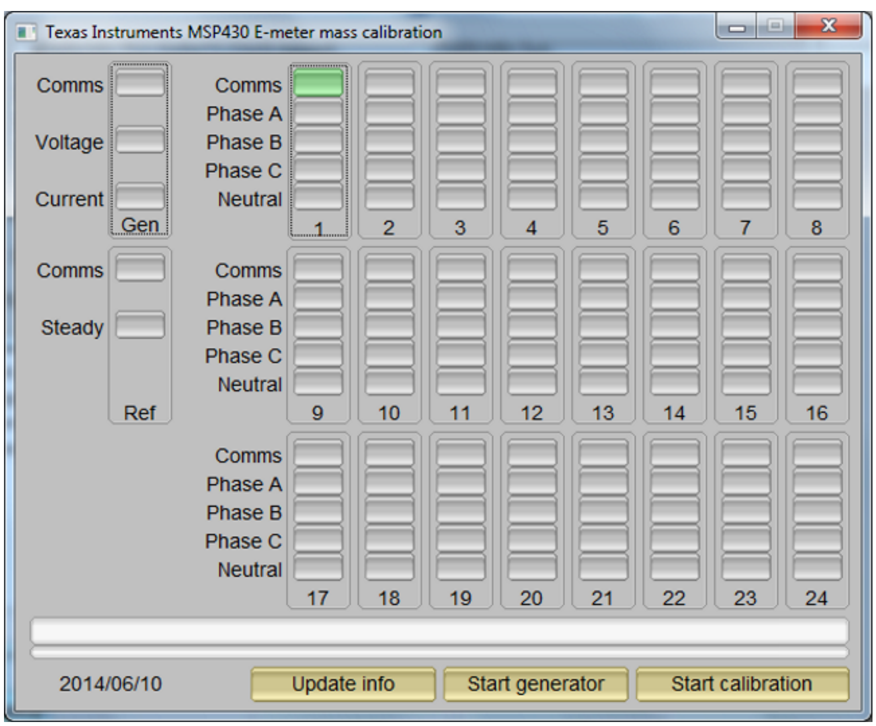

Figure 34. GUI Startup Window

Upon clicking on the green button, the results window opens (see Figure 35). In the figure, there is a trailing "L" or "C" on the Power factor values to indicate an inductive or capacitive load, respectively.

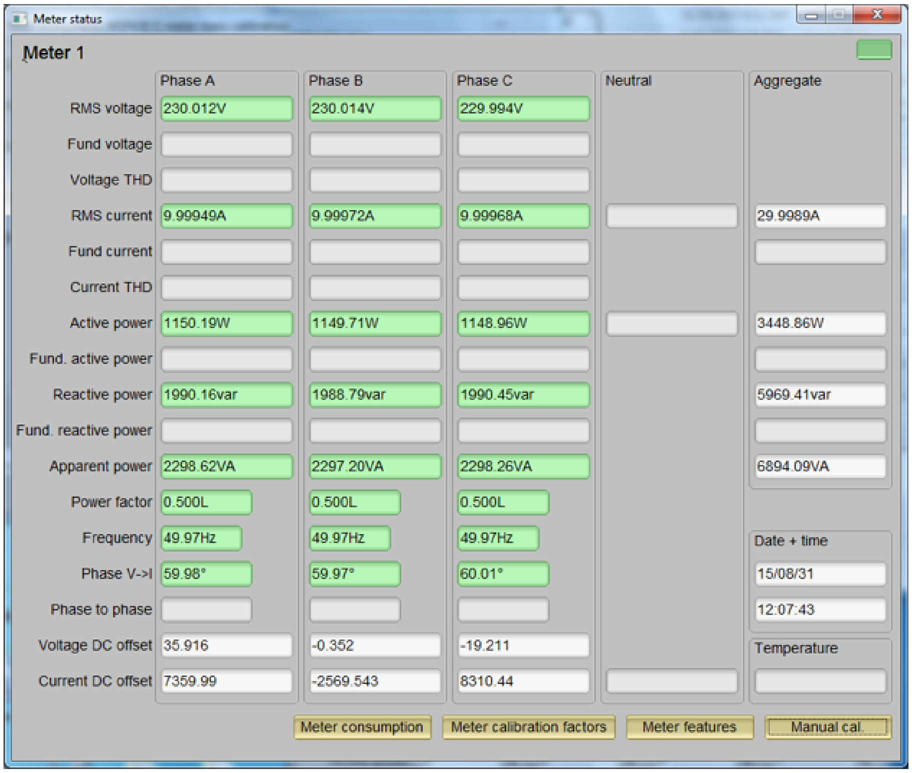

Figure 35. GUI Results Window

From the results window, the total energy consumption readings and sag and swell logs can be viewed by clicking the "Meter consumption" button. After the user clicks this button, the Meter events and consumption window pops up, as Figure 36 shows.

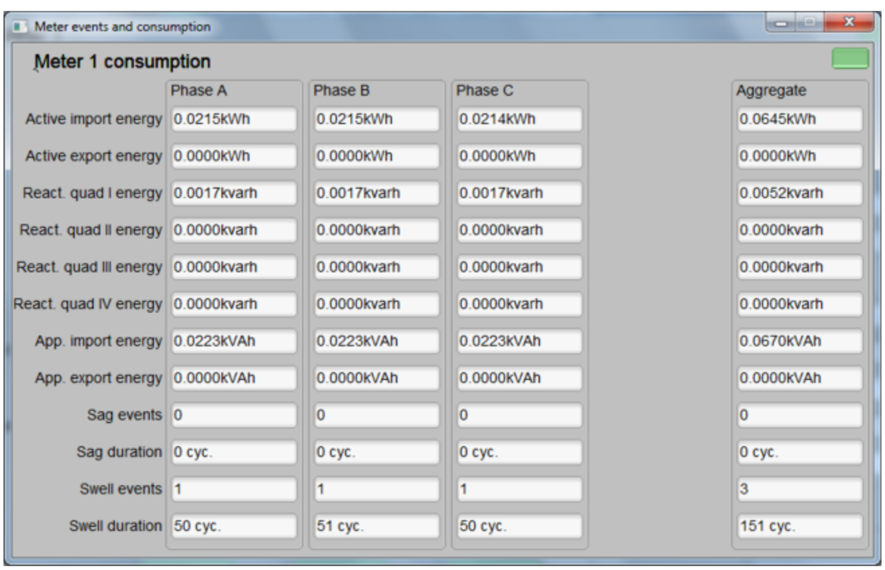

Figure 36. Meter Events and Consumption Window

From Figure 36, the user can view the meter settings by clicking the "Meter features" button, view the system calibration factors by clicking the "Meter calibration factors" button, or open the window used for calibrating the system by clicking the "Manual cal." button.

7.2.2 Calibration

Calibration is key to any meter performance and it is absolutely necessary for every meter to go through this process. Initially, every meter exhibits different accuracies due to silicon-to-silicon differences, sensor accuracies, and other passive tolerances. To nullify these effects, every meter must be calibrated. To perform calibration accurately there should be an accurate AC test source and a reference meter available. The source must be able to generate any desired voltage, current, and phase shifts (between V and I). To calculate errors in measurement, the reference meter acts as an interface between the source and the meter being calibrated. This section discusses a simple and effective method of calibration of this three-phase EVM.

The GUI used for viewing results can easily be used to calibrate the EVM. During calibration, parameters called calibration factors are modified in software to give the least error in measurement. For this meter, there are six main calibration factors for each phase: voltage scaling factor, voltage AC offset, current scaling factor, current AC offset, power scaling factor, and the phase compensation factor. The voltage, current, and power scaling factors translate measured quantities in metrology software to real-world values represented in volts, amps, and watts, respectively. The voltage AC offset and current AC offset eliminate the effect of additive white Gaussian noise (AWGN) associated with each channel. This noise is orthogonal to everything except itself; as a result, this noise is only present when calculating RMS voltages and currents. The last calibration factor is the phase compensation factor, which compensates any phase shifts introduced by the current sensors and other passives. Note that the voltage, current, and power calibration factors are independent from each other. Therefore, calibrating voltage does not affect the readings for RMS current or power.

When the meter SW is flashed with the code (available in the *.zip file), default calibration factors are loaded into these calibration factors. These values are to be modified through the GUI during calibration. The calibration factors are stored in INFO_MEM, and therefore, remain the same if the meter is restarted. However, if the code is re-flashed during debugging, the calibration factors are replaced and the meter has to be recalibrated. One way to save the calibration values is by clicking on the Meter calibration factors button (see Figure 35). The Meter calibration factors window (see Figure 37) displays the latest values, which can be used to restore calibration values.

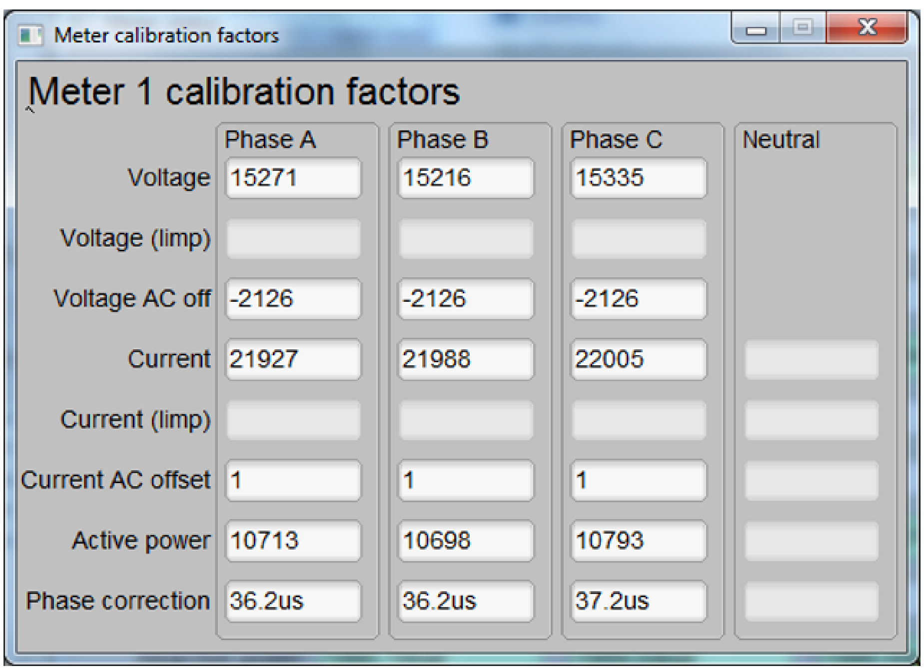

Figure 37. Calibration Factors Window

Calibrating any of the scaling factors is referred to as gain correction. Calibrating the phase compensation factors is referred to as phase correction. For the entire calibration process, the AC test source must be ON, meter connections consistent with Section 4.1, and the energy pulses connected to the reference meter.

7.2.2.1 Gain Calibration

Usually gain correction for voltage and current can be done simultaneously for all phases. However, energy accuracy (%) from the reference meter for each individual phase is required for gain correction for active power. Also, when performing active power calibration for any given phase, the other two phases must be turned OFF. Typically, switching only the currents OFF is good enough for disabling a phase.

7.2.2.1.1 Voltage and Current Gain Calibration

To calibrate the voltage and current readings, perform the following steps:

1. Connect the GUI to view results for voltage, current, active power, and the other metering parameters.
2. Configure the test source to supply desired voltage and current for all phases. Ensure that these are the voltage and current calibration points with a zero-degree phase shift between each phase voltage and current. For example, for 230 V, 10 A, 0º (PF = 1). Typically, these values are the same for every phase.
3. Click on the "Manual cal." button that Figure 35 shows. The following screen pops up from Figure 38:

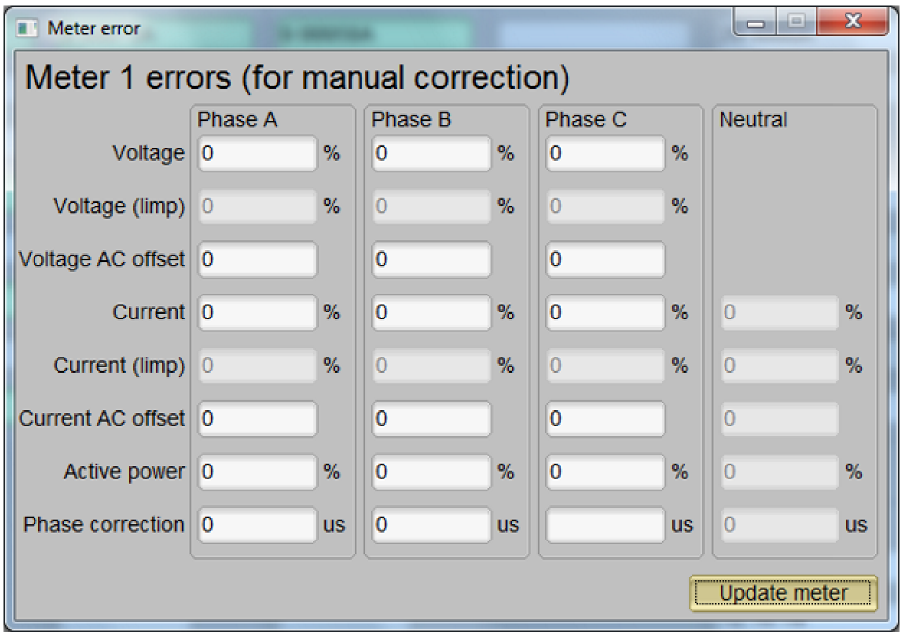

Figure 38. Manual Calibration Window

4. Calculate the correction values for each voltage and current. The correction values that must be entered for the voltage and current fields are calculated by:

$$\text{Correction}\,(\%) = \left(\frac{\text{value}_{\text{observed}}}{\text{value}_{\text{desired}}} - 1\right) \times 100 \tag{21}$$

   where
   - $\text{value}_{\text{observed}}$ is the value measured by the TI meter
   - $\text{value}_{\text{desired}}$ is the calibration point configured in the AC test source.
5. After calculating for all voltages and currents, input these values as is (±) for the fields Voltage and Current for the corresponding phases.
6. Click on the "Update meter" button and the observed values for the voltages and currents on the GUI settle to the desired voltages and currents.

7.2.2.1.2 Active Power Gain Calibration

NOTE: This example is for one phase. Repeat these steps for other phases.

After performing gain correction for voltage and current, gain correction for active power must be done. Gain correction for active power is done differently in comparison to voltage and current. Although, conceptually, calculating using Step 4 with active power readings (displayed on the AC test source) can be done, this method is not the most accurate and should be avoided.

The best option to get the Correction % is directly from the reference meters measurement error of the active power. This error is obtained by feeding energy pulses to the reference meter. To perform active power calibration, perform the following steps:

1. Turn off the system and connect the energy pulse output of the system to the reference meter. Configure the reference meter to measure the active power error based on these pulse inputs.
2. Turn on the AC test source.
3. Repeat Step 1 to Step 3 from Section 7.2.2.1.1 with the identical voltages, currents, and 0º phase shift that were used in the same section.
4. Obtain the % error in measurement from the reference meter. Note that this value may be negative.
5. Enter the error obtained in the previous Step 4 into the Active Power field under the corresponding phase in the GUI window. This error is already the correction (%) value and does not require calculation.
6. Click on Update meter button and the error values on the reference meter immediately settle to a value close to zero.

7.2.2.2 Phase Correction

After performing power gain correction, phase calibration must be performed. Similar to active power gain calibration, to perform phase correction on one phase, the other phases must be disabled. To perform phase correction calibration, perform the following steps:

1. If the AC test source has been turned OFF or reconfigured, perform Step 1 through Step 3 from Section 7.2.2.1.1 using the identical voltages and currents used in that section.
2. Disable all other phases that are not currently being calibrated by setting the current of these phases to 0 A.
3. Modify only the phase-shift to a non-zero value; typically, 60º is chosen. The reference meter now displays a different % error for active power measurement. Note that this value may be negative.
4. If this error from Step 3 is not close to zero, or is unacceptable, perform phase correction by following these steps:
   (a) Enter a value as an update for the Phase Correction field for the phase that is being calibrated. Usually, a small ± integer must be entered to bring the error closer to zero. Additionally, for a phase shift greater than 0 (for example: 60º), a positive (or negative) error would require a positive (negative) number as correction.
   (b) Click on the Update meter button and monitor the error values on the reference meter.
   (c) If this measurement error (%) is not accurate enough, fine-tune by incrementing or decrementing by a value of 1 based on Step 4a and Step 4b. Note that after a certain point, the fine-tuning only results in the error oscillating on either side of zero. The value that has the smallest absolute error must be selected.
   (d) Change the phase now to −60° and check if this error is still acceptable. Ideally, errors should be symmetric for same phase shift on lag and lead conditions.

After performing phase correction, calibration is complete for one phase. Note that the gain calibration and phase calibration are completed in sequence for each phase before moving on to other phases. These two procedures must be repeated for each phase, unlike voltage and current calibration.

This completes calibration of voltage, current, and power for all three phases. View the new calibration factors (see Figure 39) by clicking the Meter calibration factors button of the GUI metering results window in Figure 35.

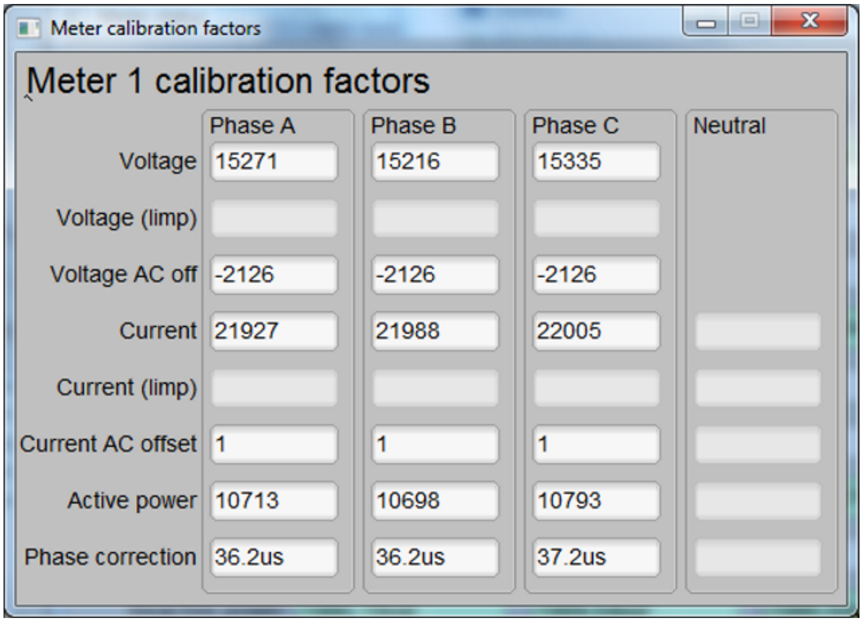

Figure 39. Calibration Factors Window

Also view the configuration of the system by clicking on the Meter features button in Figure 35 to get to the window that Figure 40 shows.

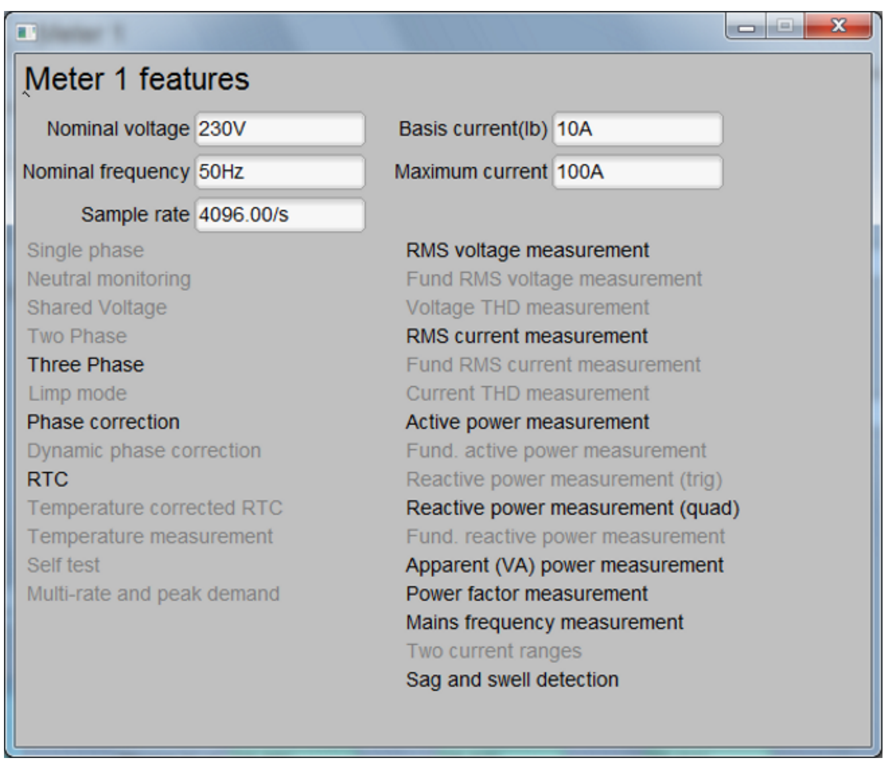

Figure 40. Meter Features Window

8 Test Data

8.1 Metrology Results

Table 5. Active Energy % Error

CURRENT (A)	0°	60°	−60°
0.05	0.021	0.046	0.016
0.1	–0.045	–0.033	–0.018
0.25	–0.008	–0.003	–0.024
0.5	–0.005	0.006	–0.003
1	0.007	0.009	0.009
2	–0.002	–0.004	–0.004
5	0.008	–0.011	0.025
10	0.008	–0.023	0.050
20	0.017	–0.031	0.059
30	0.016	–0.046	0.090
40	0.024	–0.059	0.116
50	0.020	–0.103	0.145
60	0.017	–0.113	0.157
70	0.030	–0.113	0.174
80	0.030	–0.121	0.176
90	0.029	–0.138	0.176
100	0.019	–0.143	0.176

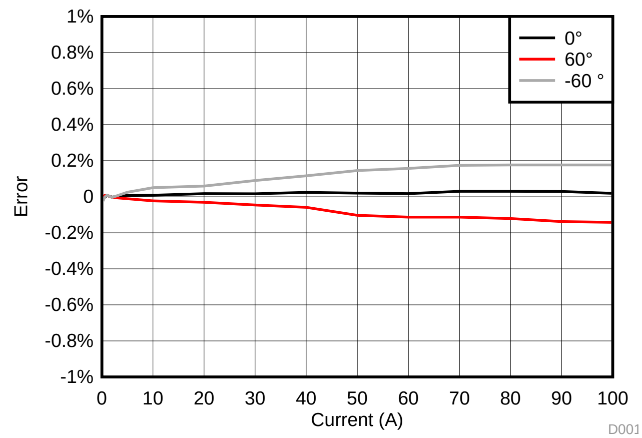

Figure 41. Active Energy % Error

Table 6. Reactive Energy % Error

CURRENT (A)	60°	−60°
0.05	–0.070	0.007
0.1	–0.075	–0.002
0.25	–0.050	–0.017
0.5	–0.034	–0.031
1	–0.032	–0.026
2	–0.049	–0.036
5	–0.036	–0.036
10	–0.017	–0.031
20	–0.024	–0.031
30	–0.003	–0.034
40	0.012	–0.046
50	0.003	–0.042
60	0.012	–0.049
70	0.027	–0.048
80	0.019	–0.062
90	0.042	–0.030
100	0.045	–0.032

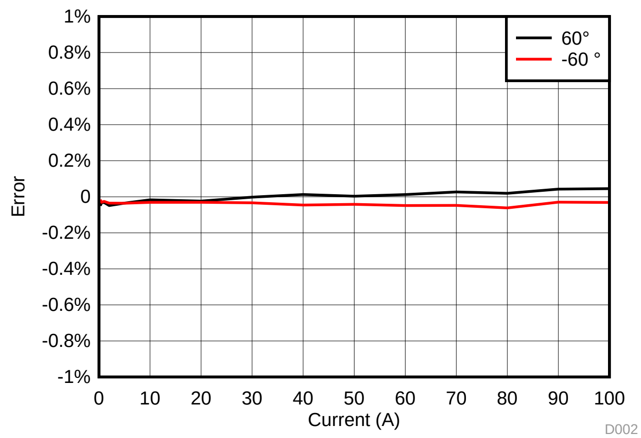

Figure 42. Reactive Energy % Error

The results from this test show that the MSP430F67791A can meet class 0.2% accuracy.

8.2 Current Consumption Testing

Table 7 through Table 10 show the peak current and duration of different regions for the cases the chip is powered from DVCC and AUXVCC1 as well as the cases where magnetic tampering is currently detected and when it is currently not being detected. When running from DVCC, the upper bound for the average current is less than 20 µA per sensor, which is negligible because DVCC would be powered from mains. In case DVCC is not available and the system is running from AUXVCC1, the upper bound of the current consumption per device is reduced to less than 2 µA per sensor.

Table 7. Region Peak Current and Duration, DVCC, Current Magnetic Tampering Not Present

REGION NUMBER	PEAK MEASURED VOLTAGE	DURATION	CALCULATED PEAK CURRENT
1	304 mV	36 µs	6204 µA
2	136 mV	224 µs	2776 µA
3	0 mV	41340 µs	0

Total duration = 36 µs + 224 µs + 41340 µs = 41600 µs

Upper bound for average current of set of Hall sensors = (6204 × 36 + 2776 × 224 + 0 × 41340) / 41600 = 20.32 µA

Upper bound for average current of Hall sensor = 20.32 µA / 3 = 6.77 µA

Table 8. Region Peak Current and Duration, DVCC, Current Magnetic Tampering is Present

REGION NUMBER	PEAK MEASURED VOLTAGE	DURATION	CALCULATED PEAK CURRENT
1	376 mV	260 µs	7673 µA
2	0 mV	41340 µs	0

Total duration = 260 µs + 41340 µs = 41600 µs

Upper bound for average current of set of Hall sensors = (7673 × 260 + 0 × 41340) / 41600 = 47.95 µA

Upper bound for average current of Hall sensor = 47.95 µA / 3 = 15.99 µA

Table 9. Region Peak Current and Duration, AUXVCC1, Current Magnetic Tampering Not Present

REGION NUMBER	PEAK MEASURED VOLTAGE	DURATION	CALCULATED PEAK CURRENT
1	148 mV	16 µs	14800 µA
2	84 mV	48 µs	8400 µA
3	0 mV	249936 µs	0

Total duration = 16 µs + 48 µs + 49936 µs = 250000 µs

Upper bound for average current of set of Hall sensors
= (14800 × 16 + 8400 × 48 µs + 0 × 249936 µs) / 250000 µs = 2.56 µA

Upper bound for average current of Hall sensor = 2.56 µA / 3 = 0.853 µA

Table 10. Region Peak Current and Duration, AUXVCC1, Current Magnetic Tampering is Present

REGION NUMBER	PEAK MEASURED VOLTAGE	DURATION	CALCULATED PEAK CURRENT
1	208 mV	16 µs	20800 µA
2	104 mV	60 µs	10400 µA
3	0 mV	249924 µs	0

Total duration = 16 µs + 60 µs + 249924 µs = 250000 µs

Upper bound for average current of set of Hall sensors
= (20800 × 16 + 10400 × 60 + 0 × 249924) / 250000 = 3.83 µA

Upper bound for average current of Hall sensor = 20.32 µA / 3 = 1.2757 µA

9 Design Files

9.1 Schematics

To download the schematics, see the design files at TIDA-00839.

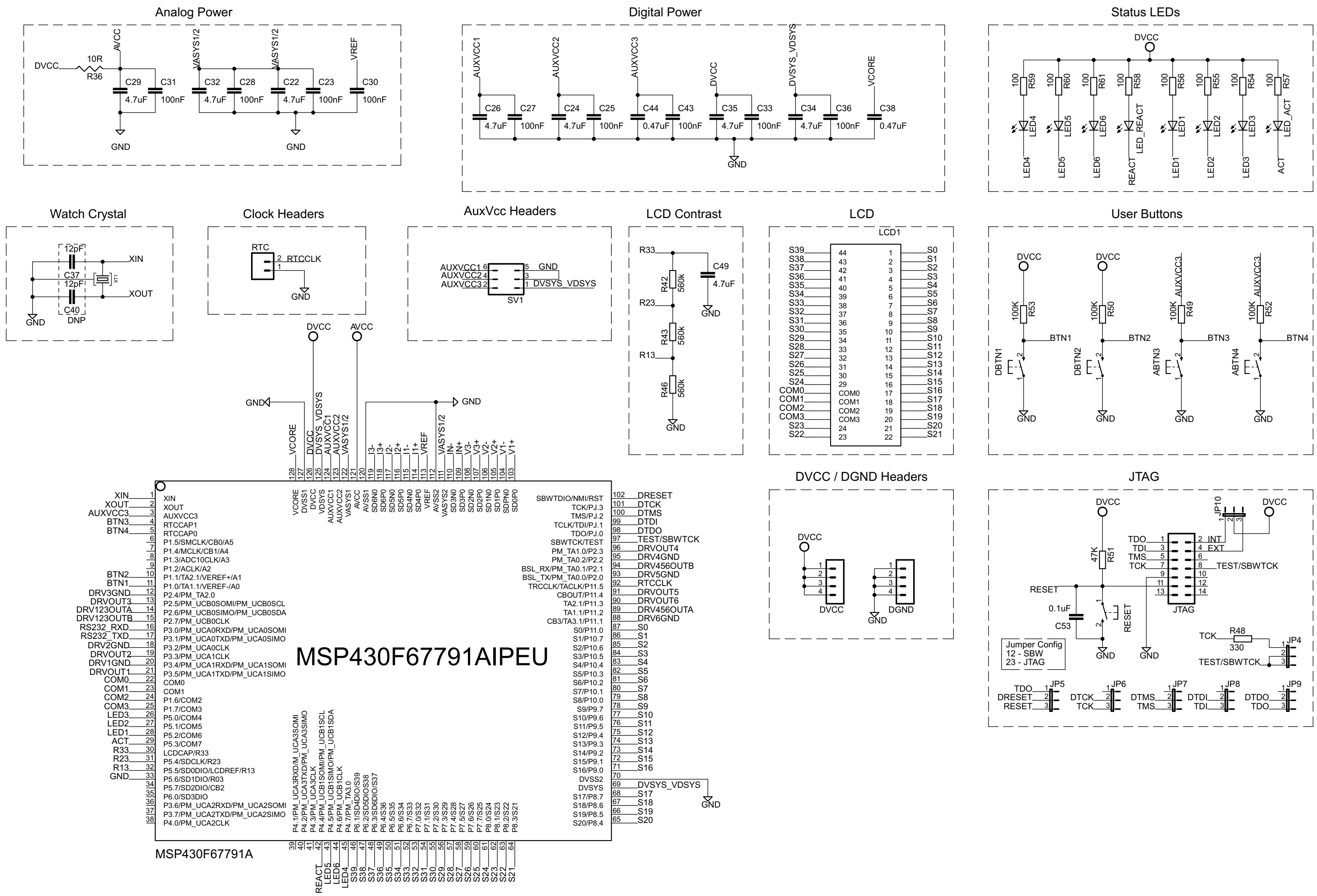

Figure 43. TIDA-00839 Schematics Page 1

Analog Front-End (Current) / Analog Front-End (Voltage)

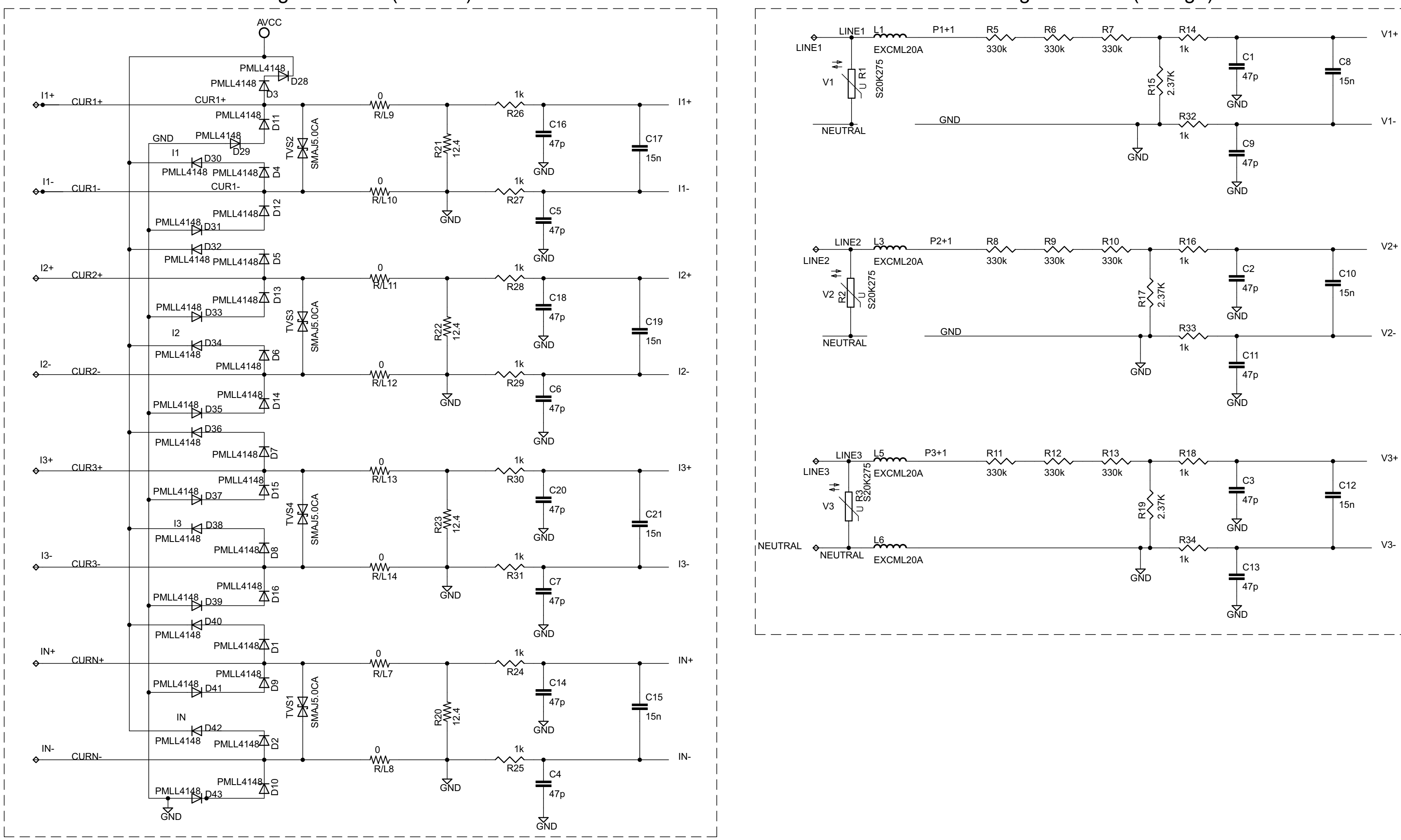

Figure 44. TIDA-00839 Schematics Page 2

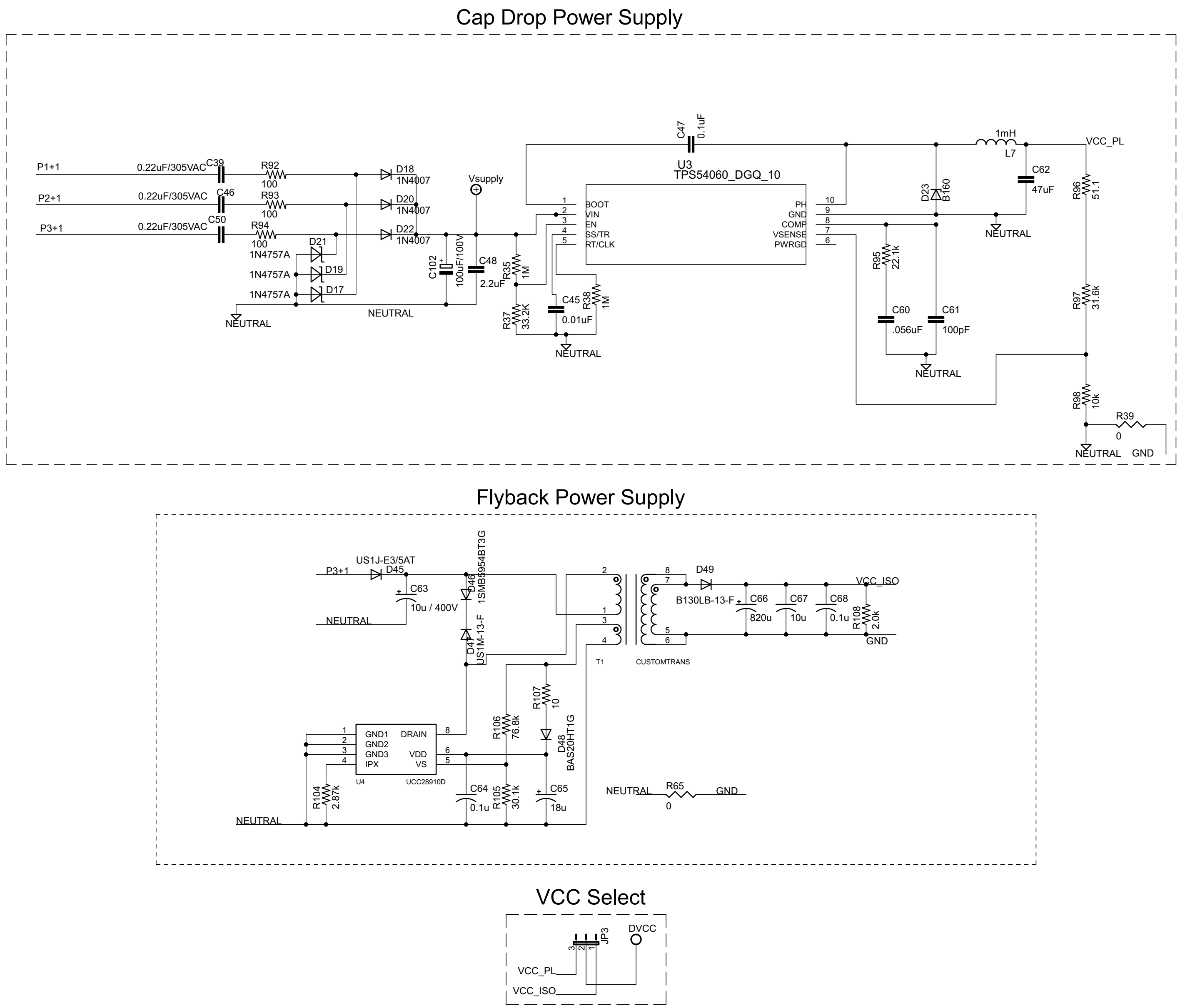

Figure 45. TIDA-00839 Schematics Page 3

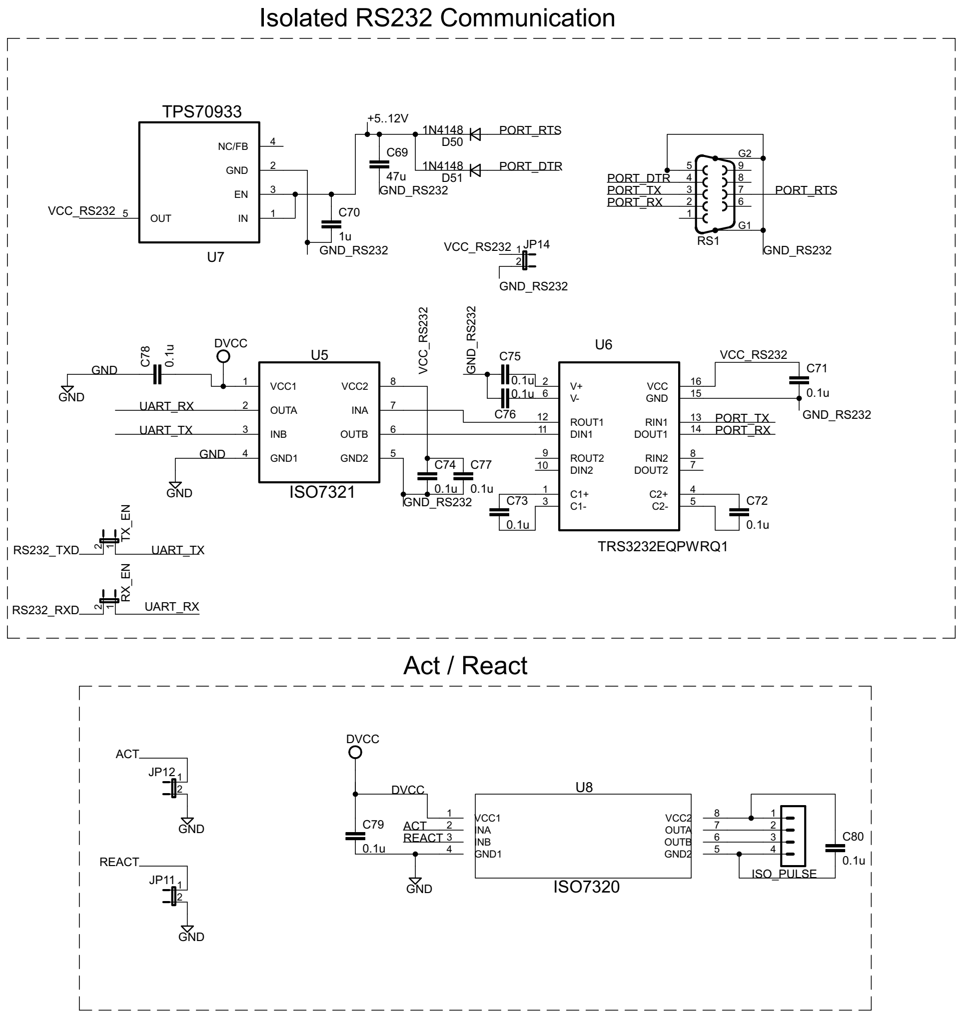

Figure 46. TIDA-00839 Schematics Page 4

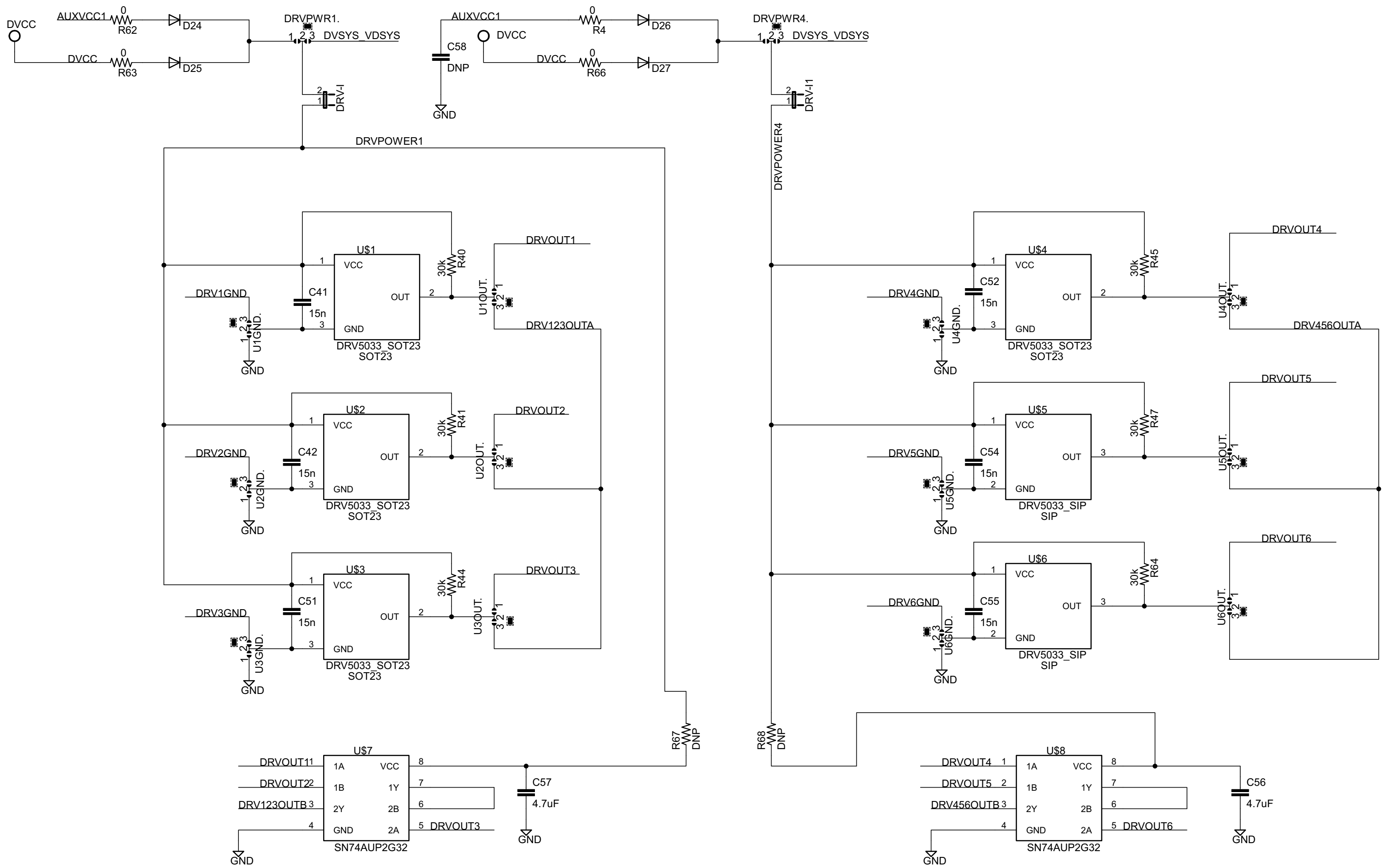

Figure 47. TIDA-00839 Schematics Page 5

9.2 Bill of Materials

To download the bill of materials (BOM), see the design files at TIDA-00839.

9.3 PCB Layout Recommendations

- Use ground planes instead of ground traces where possible and minimize the cuts in these ground planes (especially for critical traces) in the direction of current flow. Ground planes provide a low-impedance ground path which minimizes induced ground noise. However, cuts in the ground plane can increase inductance. If there are cuts in the ground plane, they should be bridged on the opposite side with a 0-Ω resistor.
- When there is a ground plane on both top and bottom layers of a board (such as in our EVM), ensure there is good stitching between these planes through the liberal use of vias that connect the two planes.
- Keep traces short and wide to reduce trace inductance.
- Use wide VCC traces and star-routing for these traces instead of point-to-point routing.
- Isolate sensitive circuitry from noisy circuitry. For example, high voltage and low voltage circuitry should be separated.
- Use decoupling capacitors with low effective series resistance (ESR) and effective series inductance. Place decoupling capacitors close to their associated pins.
- Minimize the length of the traces used to connect the crystal to the microcontroller. Place guard rings around the leads of the crystal and ground the crystal housing. In addition, there should be clean ground underneath the crystal and placing any traces underneath the crystal should be prevented. Also, keep high frequency signals away from the crystal.

9.3.1 Layer Plots

To download the layer plots, see the design files at TIDA-00839.

9.4 CAD Project

To download the CAD project files, see the design files at TIDA-00839.

9.5 Gerber Files

To download the Gerber files, see the design files at TIDA-00839.

10 Software Files

To download the software files, see the design files at TIDA-00839.

11 References

1. Texas Instruments, *Sub-Microamp, Intelligent Hall-Effect Sensing Delivers 20-Year Battery Life*, White Paper (SLYY058).

12 About the Author

MEKRE MESGANAW is a Systems Engineer in the Smart Grid and Energy group at Texas Instruments, where he primarily works on grid monitoring customer support and reference design development. Mekre received his bachelor of science and master of science in computer engineering from the Georgia Institute of Technology.

Mailing Address: Texas Instruments, Post Office Box 655303, Dallas, Texas 75265